Applying Write-Once Memory Codes to Binary Symmetric Asymmetric Multiple Access Channels

School of Information Science,
Japan Advanced Institute of Science and Technology

Ryota Sekiya

March, 2016

Master Thesis

Applying Write-Once Memory Codes to Binary Symmetric Asymmetric Multiple Access Channels

1310036 Ryota Sekiya

Supervisor	Brian Kurkoski
Main Examiner	Brian Kurkoski
Examiners	Tadashi Matsumoto
	Mineo Kaneko

School of Information Science,
Japan Advanced Institute of Science and Technology

February, 2016

Abstract

Write-once memory (WOM) is a form of digital memory for the permanent storage of information. WOM codes were first designed by Rivest and Shamir, which allows reuse of such that WOM. Our work is inspired in part by application of WOM codes to reducing read latency in memories. We focus on applying WOM codes to a specific asymmetric multiple access channel (AMAC) noise model called the binary symmetric AMAC (BS-AMAC). The AMAC is a kind of the multiple access channel (MAC), which consists of two users simultaneously communicate over one common channel, however User 2 observes User 1 message.

At one specific rate pair, WOM codes can achieve the BS-AMAC maximum sum-rate. Further, any achievable rate pairs for a two-write WOM code are also an achievable rate pair for the BS-AMAC.

Numerous schemes for joint iterative decoding of two transmitted codewords at the receiver have been proposed. Successive interference cancellation is another well-known technique, however requires interaction between two decoders. Our scheme applying WOM codes to the BS-AMAC, which reduces the size of the achievable rate region, however induces effective decoding schemes: (1) symbol-wise estimation and (2) a posteriori decoding, without using joint iterative decoding or successive interference cancellation. Achievable rates of our system using two decoding schemes are also given. These two decoding schemes are effective in cooperative wireless communications despite the fact that WOM codes are designed for data storage.

In order to build more reliable communication system, some capacity-approaching error correcting codes such as low-density parity check codes (LDPC) are needed. In our work, we applied the well-known DVB-S.2 LDPC codes to our system in order to approach the BS-AMAC capacity. A bit error rate (BER) performance of our system using a LDPC code is shown.

We also briefly discuss how the AMAC model can be applied to the relay channel.

key words: *asymmetric multiple access channel, data storage code, write-once memory code, capacity, achievable rate region*

I certify that ideas, data and so on in this Master thesis are not plagiarized from other articles.

February, 2016
Ryota Sekiya

Acknowledments

First of all, I would like to express the deepest appreciation to my supervisor, Brian M. Kurkoski for his advice, assistance, discussions and persistent help during my Master study. Further, I want to thank him for giving me a lot of opportunities to contribute paper and improve English skills.

I would like to offer my special thanks to Prof. Tad Matsumoto. His supports, suggestions, and comments were invaluable in taking a larger view in the research field.

I owe a very important debt to Erick Christian Garcia Alvarez. The APP decoder part of our work was accomplished by his work. He also gave me constructive comments and warm encouragement to advance my research.

Finally, I gratefully acknowledge all the members in Matsumoto and Kurkoski laboratory for their kindly helps. My everyday through being exposed to various countries and values, was exciting and vary.

Contents

Chapter 1

Introduction

1.1 Introduction

A discrete memoryless multiple access channel (MAC), such as the up-link in wireless communication, has multiple senders and one receiver. In this model, these users share a common channel. The capacity region for this channel is well-known [1].

A two-user (discrete memoryless) asymmetric multiple access channel (AMAC) is similar to a two-user MAC, however User 1's message is known to the both users, while User 2's message is known only to User 2. De Bruyan, Prelov and van der Meulen gave the capacity region, and showed that when the messages are correlated, that source-coding separation holds [3] (in contrast to Cover et al's result on non-separability for the MAC [4]), see also [5].

A write-once medium is a form of digital memory for the storage of information (e.g. flash memory, punch cards, CD-ROMs). A write-once medium has an array of bits with two possible states, which are initially in the zero state, and which can be independently but irreversibly transformed into the one state. Write-once memory (WOM) codes were first designed and introduced for such data storage applications by Rivest and Shamir. A WOM coding scheme allows reusing a write-once medium multiple times by encoding to a recorded bit sequence and by observing the state of the medium before determining how to update the contents of the memory with new bit sequence [6].

In our research, we focus on applying WOM codes to an AMAC. Our work is inspired in part by the application of WOM codes to reducing read latency in memories [9].

We consider a specific AMAC channel called the *binary symmetric AMAC (BS-AMAC)* with binary inputs, which pass through independent binary symmetric channels (BSC). At one specific rate pair, WOM codes can achieve a point on the boundary of the BS-AMAC capacity region. Further, any achievable rate pairs for a two-write WOM code are achievable for the (two-user) BS-AMAC. Applying WOM codes to the BS-AMAC reduces the size of the achievable rate region, however induces effective decoding techniques. One decoding method is performed using symbol-wise estimation, resulting in a decomposition to two distinct channels. Achievable rates for this decomposed system are given. Another decoding method is done using a posteriori probability (APP) decoding. The maximum sum-rate of this scheme is also given.

Numerous schemes for joint iterative decoding of two transmitted codewords at the receiver (e.g. LDPC codes for the MAC [8]) have been proposed. Successive interference cancella-

tion is another well-known technique, however requires interaction between two decoders. The proposed scheme aims to efficiently separate the two codewords at the receiver, without using joint iterative decoding or successive interference cancellation. This low-complexity approach is appealing for computationally-constrained applications. In practical communication, the channel is noisy. Thus, we apply an error correcting code, LDPC code,in order to approach the BS-AMAC capacity. The bit error rate (BER) of our system using LDPC code is also given.

We also briefly discuss how the AMAC model can be applied to practical communications.

1.2 Preliminary

This section describes most of the basic definition required for our research. The preliminaries are defined in [1].

1.2.1 Entropy

Entropy is the uncertainty of random variables. Let X be a discrete random variable with alphabet $\mathcal{X}$ and probability function $p(x) = Pr\{X = x\}$, $x \in \mathcal{X}$.

Definition 1.2.1 The entropy $H(X)$ of a discrete random variable X is defined by

$$H(X) = -\sum_{x \in \mathcal{X}} p(x) \log_2 p(x). \tag{1.1}$$

Note that $0 \log_2 0 = 0$, which is easily justified by continuity since $x \log_2 x \to 0$ as $x \to 0$. Adding terms of zero probability does not change the entropy.

1.2.2 Mutual Information

Mutual information is a measure of the measure of the amount of information that one random variable contains about another random variable. It is the reduction in the uncertainty of one random variable due to knowledge of the other.

Definition 1.2.2 Consider two random variables X and Y with a joint probability mass function $p(x, y)$ and marginal probability mass function $p(x)$ and p(y). The *mutual information* $I(X; Y)$ is the relative entropy between the joint distribution and the product distribution $p(x)p(y)$:

$$I(X; Y) = \sum_{x \in \mathcal{X}} \sum_{y \in \mathcal{Y}} p(x, y) \log_2 \frac{p(x, y)}{p(x)p(y)} \tag{1.2}$$

$$= H(X) - H(X|Y). \tag{1.3}$$

1.2.3 Channel Capacity

The mathematical analog of a physical signaling system is shown in Fig.1.1. Source symbols from some finite alphabet are mapped into some sequence of channel symbols, which then

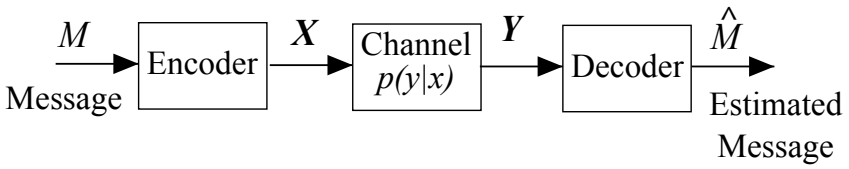

Fig. 1.1 Communication sytsem.

produces the output sequence of the channel. The output sequence is random, however has a distribution that depends on the input sequence. From the output sequence, we attempt to recover the transmitted message.

Each of the possible input sequences induces a probability distribution on the output sequences. Since two different input sequences may give rise to the same output sequence, the inputs are confusable. we show that we can choose a "non-confusable" subset of input sequences so that with high probability there is only one highly likely input that could have caused the particular output. We can then reconstruct the input sequences at the output with a negligible probability of error. By mapping the source into the appropriate "widely spaced" input sequences to the channel, we can transmit a message with very low probability of error and reconstruct the source message at the output. The maximum rate at which this can be done is called the capacity of the channel.

Definition 1.2.3 Let a *discrete channel* be a system consisting of an input alphabet $\mathcal{X}$ and output alphabet $\mathcal{Y}$ and a probability transition matrix $p(y|x)$ which denotes the probability of observing the output symbol y given that we sed the symbol x. The channel is said to be *memoryless* if the probability distribution of the output depends only on input at that time and is conditionally independent of previous channel inputs or outputs.

Definition 1.2.4 The (information) *channel capacity* of a discrete memoryless channel as:

$$C = \max_{p(x)} I(X;Y) \tag{1.4}$$

where the maximum is taken over all possible input distributions $p(x)$. Finally, the channel capacity is defined as the highest rate in bits per channel use at which information can be sent with arbitrarily low probability of error.

1.2.4 Data-processing Inequality

Theorem 1.2.1 [1] if $X \to Y \to Z$, then $I(X;Y) \leq I(X;Z)$.

Chapter 2

Asymmetric Multiple Access Channel

This chapter describes the *asymmetric multiple access channel (AMAC)* channel model used in our research. AMAC is a kind of multiple access channel (MAC). The MAC is a communication model where there some senders and one receiver, however they communicate over a common channel. This chapter mainly treats two-user MAC and AMAC, and shows their capacity.

2.1 Multiple Access Channel

Definition 2.1.1 A (discrete memoryless two-user) MAC consists of three alphabets $\mathcal{X}^1, \mathcal{X}^2$, and $\mathcal{Y}$, and a probability transition matrix $p(y|x^1, x^2)$, where $x^1 \in \mathcal{X}^1$, $x^2 \in \mathcal{X}^2$ are channel inputs from each user, and $y \in \mathcal{Y}$ is a channel output. A MAC is memoryless if

$$\begin{aligned} &P(y_1, ..., y_n|x_1^1, x_2^1, ..., x_n^1, x_1^2, x_2^2, ..., x_n^2) \\ &\qquad = \prod_{k=1}^{n} p(y_k|x_k^1, x_k^2) \end{aligned} \tag{2.1}$$

where x_k^1, x_k^2 and y_k denote the k-th input symbols and output symbol .

A $(2^{nR_1}, 2^{nR_2}, n, P_n)$ code for the (discrete memoryless) MAC is a pair of message sets and encoding functions for User 1:

$$f_1 : \{1, 2, .., 2^{nR_1}\} \to (\mathcal{X}^1)^n,$$

and for User 2:

$$f_2 : \{1, 2, .., 2^{nR_2}\} \to (\mathcal{X}^2)^n,$$

and for a MAC channel output, a decoding function g:

$$g : \mathcal{Y}^n \to (\mathcal{X}^1)^n \times (\mathcal{X}^2)^n.$$

There are two senders and one receiver for this channel. In this channel, these two users are sharing the common channel pictured in Fig. 2.1. User 1 chooses an index U^1 uniformly

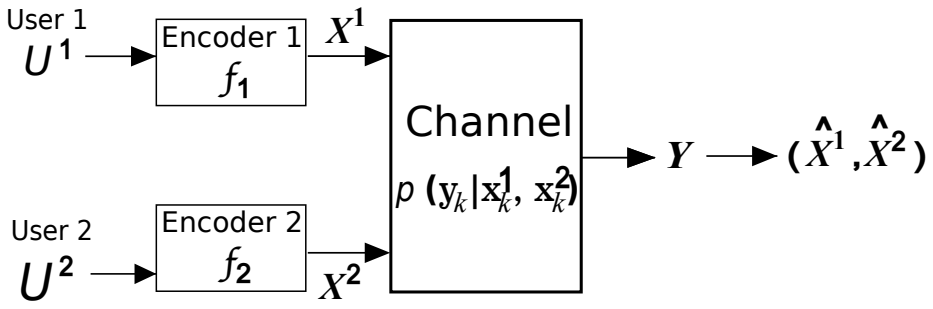

Fig. 2.1 Discrete memoryless two-user Multiple Access Channel

from the set $u^1 \in \{1, 2, ..., 2^{nR_1}\}$ and sends the corresponding codeword over the channel. User 2 does likewise [1].

The probability of error $P_{error}^{(n)}$ of this code is defined as:

$$P_{error}^{(n)} = P\Big\{g(Y^n) \neq (U^1, U^2)\Big\}, \tag{2.2}$$

A pair of rates (R_1, R_2) is said to be an *achievable rate*, if there exists a sequence $(2^{nR_1}, 2^{nR_2}, n, P_{error}^{(n)})$ codes with $P_{error}^{(n)} \to 0$ as $n \to \infty$.

2.2 Capacity Region of MAC

The definition of the capacity region of the MAC is defined in [1] and satisfies the following theorem,

Theorem 2.2.1 The *capacity region* of the MAC $(\mathcal{X}^1 \times \mathcal{X}^2, p(y|x^1, x^2), \mathcal{Y})$ is the closure of the convex hull of the set of all achievable rates (R_1, R_2) satisfying:

$$R_1 \leq I\left(X^1; Y|X^2\right), \tag{2.3}$$

$$R_2 \leq I\left(X^2; Y|X^1\right), \tag{2.4}$$

$$R_1 + R_2 \leq I\left(X^1, X^2; Y\right), \tag{2.5}$$

for the joint input distribution $p(x^1)p(x^2)$ on $\mathcal{X}^1 \times \mathcal{X}^2$.

The capacity region of the MAC is illustrated in Fig. 2.2. An investigation of the pentagon region in Fig. 2.2 is given by [1] as follows:

The point A corresponds to the maximum rate achievable from User 1 to the receiver while User 2 is not sending any information, thus

$$\max R_1 = \max_{p(x^1)p(x^2)} I(X^1; Y|X^2). \tag{2.6}$$

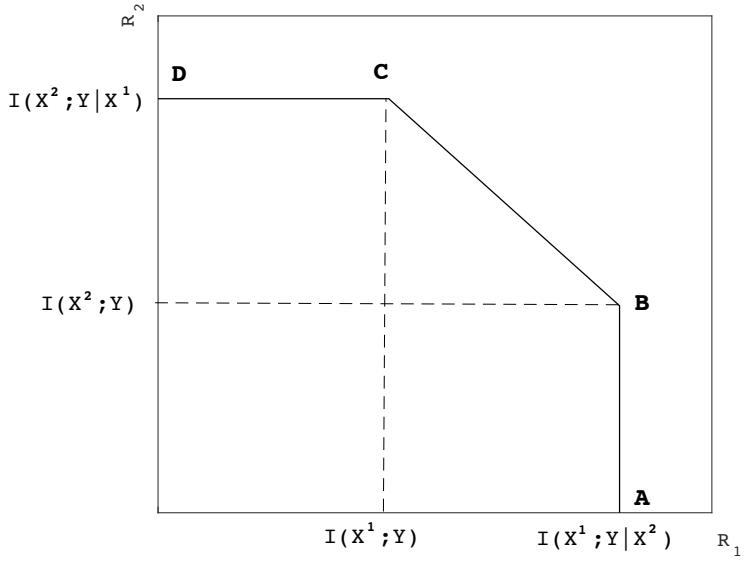

Fig. 2.2 Capacity region of the MAC

For any distribution $p(x^1)p(x^2)$

$$\begin{aligned} I(X^1;Y|X^2) &= \sum_{x^2} p(x^2) I(X^1;Y|X^2=x^2), \\ &\le \max_{x^2} I(X^1;Y|X^2=x^2), \end{aligned} \tag{2.7}$$

Therefore, the max R_1 in (2.6) is attained when we set $X^2 = x^2$, which maximizes the conditional mutual information between X^1 and Y. The distribution of X^1 is chosen to maximize this mutual information. Thus, X^2 must facilitate the transmission of X^1 by setting $X^2 = x^2$.

The point B ($R_1 = I(X^1;Y|X^2), R_2 = I(X^2;Y)$) corresponds to the maximum rate of User 2 while User 1 sends at its maximum rate. This rate is obtained if X^1 is considered as noise for the channel from X^1 to Y. In this case, X^2 can send at a rate $I(X^2;Y)$ if over a single-user channel. Since, the receiver knows which X^2 codeword was used, it can decode the codewords from User 2 with small error probability, and "subtract" its effect from the channel. We can consider the channel to be an indexed series of single-user channels, where the index is the X^2 symbol used. The rate of User 1 is achieved by taking the average mutual information over these channels, and each channel occurs as many times as the corresponding X^2 symbol in the codewords. Thereby, the rate R_1 is

$$\sum_{x^2} p(x^2) I(X^1;Y|X^2=x^2) = I(X^1;Y|X^2). \tag{2.8}$$

The points C and D correspond to B and A, respectively, however the roles of User 1 and User 2 are reversed. The non-corner points on the boundary can be achieved by time-sharing.

2.3 Asymmetric Multiple Access Channel

This section describes the AMAC for two users, User 1 and User 2, pictured in Fig. 2.3, which is similar to a conventional two-user MAC in Sec. 2.1, with one key difference: User 2 knows the message of the User 1. A discrete memoryless AMAC consists of three alphabets $\mathcal{X}^1, \mathcal{X}^2$, and $\mathcal{Y}$, and a probability transition matrix $p(y|x^1, x^2)$.

A $(2^{nR_1}, 2^{nR_2}, n, P_n)$ code for the (discrete memoryless) AMAC is a pair of message sets and encoding functions for User 1:

$$f_1 : \{1, 2, .., 2^{nR_1}\} \to (\mathcal{X}^1)^n,$$

and for User 2:

$$f_2 : \{1, 2, .., 2^{nR_2}\} \times (\mathcal{X}^1)^n \to (\mathcal{X}^2)^n,$$

and an AMAC channel output, and a decoding function g:

$$g : \mathcal{Y}^n \to (\mathcal{X}^1)^n \times (\mathcal{X}^2)^n.$$

There are also two senders and one receiver for this channel as the MAC. User 1 chooses an index U^1 uniformly from the set $u^1 \in \{1, 2, ..., 2^{nR_1}\}$ and sends the corresponding codeword over the channel. User 2 also chooses an index U^2 uniformly from the set $u^2 \in \{1, 2, ..., 2^{nR_2}\}$, but User 2 knows the message U^1, thereby sends the corresponding codeword conditioned on knowing $f_1(U^1)$ over the common channel.

2.4 Capacity Region of AMAC

Definition 2.4.1 The *capacity region* of the AMAC $(\mathcal{X}^1 \times \mathcal{X}^2, p(y|x^1, x^2), \mathcal{Y})$ is the closure of the convex hull of the set of all achievable rates (R_1, R_2).

The restriction of the AMAC capacity has the similar property as the MAC capacity (2.3), (2.4) and (2.5). However, User 2 can observe User 1's message in the AMAC, thus the rate R_1 is released from the restriction for User 1 (2.3).

Theorem 2.4.1 [3] The capacity region of the AMAC is the set of (R_1, R_2) that satisfy:

$$R_2 \leq I\left(X^2; Y|X^1\right) \tag{2.9}$$

$$R_1 + R_2 \leq I\left(X^1, X^2; Y\right) \tag{2.10}$$

for all $p(x_1, x_2) = p(x_1)p(x_2|x_1)$.

2.5 Binary Symmetric Channel

This section describes a common noisy communication channel *binary symmetric channel (BSC)* defined in [1]. In general, communication channels do not have a simple structure,

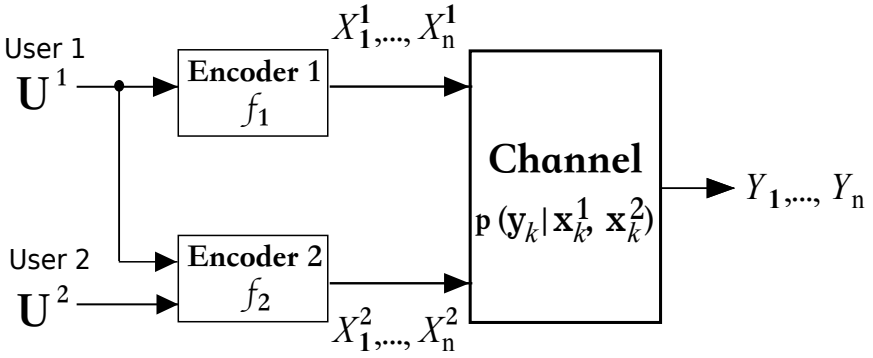

Fig. 2.3 Discrete memoryless two-user AMAC.

thus we cannot always identify a subset of the inputs to send information without error. However, if we consider a sequence of transmissions, all channels look like a BSC and we can then identify a subset of the input sequences (the codewords) that can be used to transmit information over the channel in such a way that the sets of possible output sequences associated with each of the codewords are approximately disjoint. We can then look at the output sequence and identify the input sequence with a vanishingly low probability of error.

Definition 2.5.1 [1] The binary symmetric channel is a noisy communication channel with binary input and binary output and probability of error P_e.

BSC output is equal to the input with probability $1 - P_e$. With probability P_e, on the other hand, a 0 is received as 1, and vice versa as shown in Fig. 2.4.

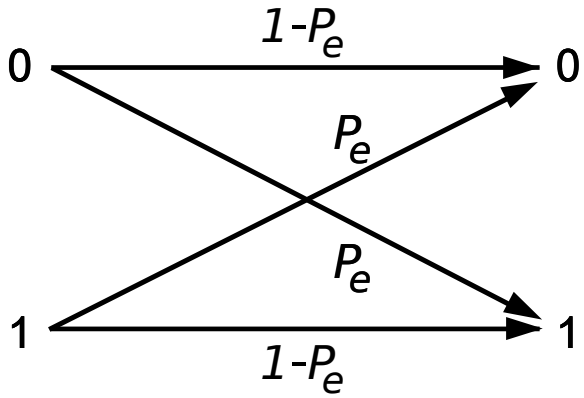

Fig. 2.4 Binary symmetric AMAC.

2.6 Binary symmetric AMAC

The BS-AMAC is a specific two-user AMAC used in our research, and is pictured in Fig. 2.5.

Definition 2.6.1 A BS-AMAC consists of five alphabets $\mathcal{X}^1, \mathcal{X}^2, \mathcal{Y}^1, \mathcal{Y}^2, \mathcal{Y}$, and a probability transition matrix $p(y|x^1, x^2)$, where each input X^i passes through a BSC with error

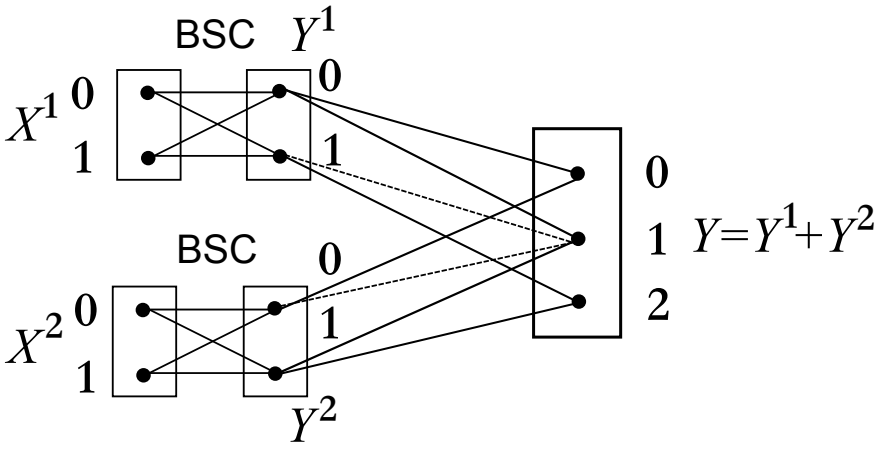

Fig. 2.5 Binary symmetric AMAC.

probability P_e, thus $Y^1 \in \mathcal{Y}^1$, $Y^2 \in \mathcal{Y}^2$ are BSC outputs for each input $\mathcal{X}^1$ and $\mathcal{X}^2$. Let $\mathcal{X}^1 = \mathcal{X}^2 = \mathcal{Y}^1 = \mathcal{Y}^2 = \{0, 1\}$. The channel output Y is the integer-valued addition of the two BSC outputs, i.e. deterministic channel $y = y^1 + y^2$, so $\mathcal{Y} = \{0, 1, 2\}$.

In the BS-AMAC, the error probability P_e of BSCs is:

$$P_e = P(Y^i \neq X^i) \ \ for \ \ i = 1, 2.$$

and conditional probability distributions $p(y^1|x^1)$, $p(y^2|x^2)$ over BSC are given by:

$$p(y^i|x^i) = \begin{cases} 1 - P_e & \text{for } x^i = y^i, \\ P_e & \text{otherwise}, \end{cases}$$

where $i = 1, 2$. Hence, a probability transition matrix follows:

$$p(y|x^1, x^2) = \sum_{y_1, y_2} p(y|y^1, y^2) p(y^1|x^1) p(y^2|x^2)$$

and is given by Table 2.1.

Table 2.1 conditional distribution $p(y|x^1, x^2)$ BS-AMAC

x^1, x^2	$Y = 0$	$Y = 1$	$Y = 2$
0, 0	$(1 - P_e)^2$	$2P_e(1 - P_e)$	P_e^2
0, 1	$(1 - P_e)P_e$	$(1 - P_e)^2$	$(1 - P_e)P_e$
1, 0	$(1 - P_e)P_e$	$(1 - P_e)^2$	$(1 - P_e)P_e$
1, 1	P_e^2	$2P_e(1 - P_e)$	$(1 - P_e)^2$

2.7 Capacity Region of BS-AMAC

The capacity region of the BS-AMAC is the closure of the convex hull of the set of all achievable rates (R_1, R_2), which satisfy (2.9) and (2.10). Note that User 2 knows User 1 message

in the AMAC, thereby both user's inputs X^1 and X^2 are jointly distributed. Accordingly, this capacity region is described using the joint input distribution $p(x^1)p(x^2|x^1)$.

We characterize this joint input distribution using three variables p_1, p_2, α as shown in Table 2.2. Here, p_1 and p_2 are defined by $p(X^1 = 1) = p_1$ and $p(X^2 = 1) = p_2$, respectively.

This parameterized joint input distribution for the BS-AMAC $p(x^1)p(x^2|x^1)$ depends on the parameter α, which is bounded as:

$$\max(0, \frac{p_1 + p_2 - 1}{p_2}) \leq \alpha \leq \min(1, \frac{p_1}{p_2}).$$

If $\alpha = p_1$, then X^1 and X^2 are independent.

Table 2.2 Joint input distribution $p(x^1, x^2)$ on $\mathcal{X}^1 \times \mathcal{X}^2$

$p(x^1, x^2)$		X^2 $x^2 = 0$	$x^2 = 1$	$p(x^1)$
X^1	$x^1 = 0$	$1 - p_1 - (1 - \alpha)p_2$	$(1 - \alpha)p_2$	$1 - p_1$
	$x^1 = 1$	$p_1 - \alpha p_2$	αp_2	p_1
	$p(x^2)$	$1 - p_2$	p_2	

We here find the BS-AMAC capacity region and *maximum sum-rate* $\max I(X^1, X^2; Y)$ with errors $P_e \geq 0$, pictured in Fig. 2.6 and in Table 2.6. The size of the region and maximum sum-rate decrease with increasing BSC error probability P_e.

Table 2.3 Maximum sum-rate $\max I(X^1, X^2; Y)$ with errors $P_e \geq 0$

P_e	0	0.01	0.02	0.03	0.04
$\max I(X^1, X^2; Y)$	1.585	1.437	1.330	1.240	1.159

0.05	0.06	0.07	0.08	0.09	0.10
1.087	1.021	0.961	0.905	0.853	0.804

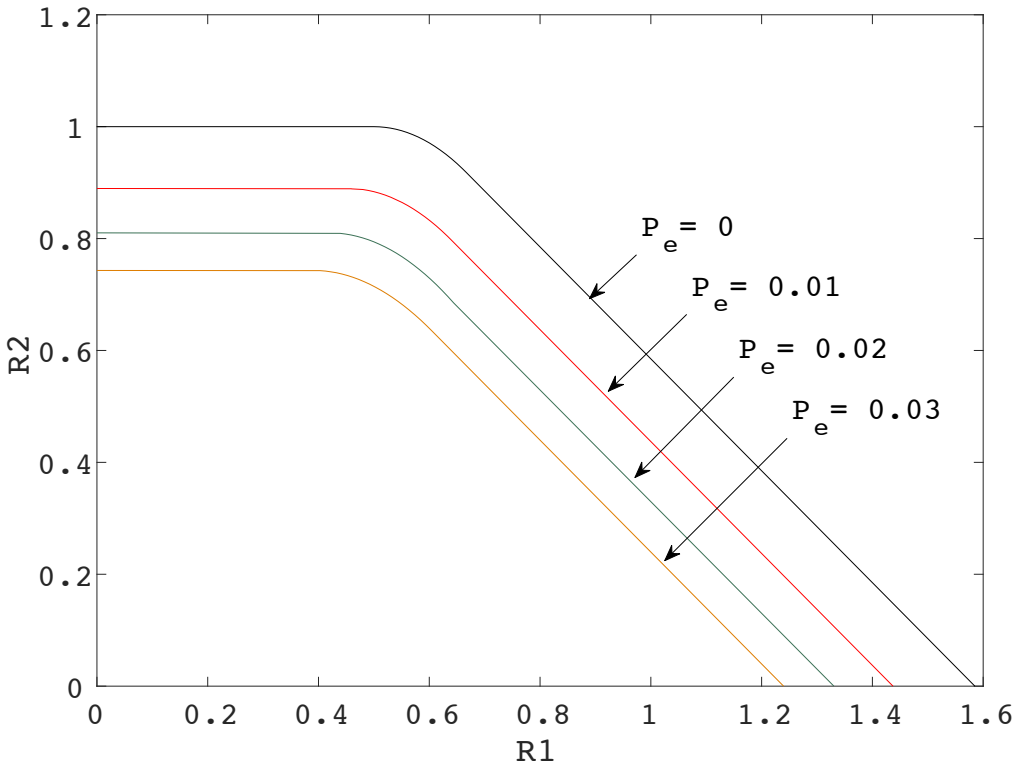

Fig. 2.6 Capacity of the BS-AMAC with error probability P_e.

Chapter 3

Write-Once Memory Code

Write-once memory (WOM) codes were first designed and introduced for write-once medium by Rivest and Shamir. This chapter describes a coding scheme WOM codes and an example (3,2) WOM codes.

3.1 Write-Once Memory

Data storage mediums have n cells used to store data bits. Every cell has two levels: 0 and 1. Cells can change only $0 \rightarrow 1$, however not vice versa. These mediums are called write-once memory (WOM), e.g. keypunch cards, paper tape, photographic film, and flash memory.

A sequence of t messages $M_1, M_2, ..., M_t$ will be written on to the WOM cells, and when M_i is written, we do not need to remember the value of the previous messages (let k_i denote the number of bits in the message M_i and let $M_i \in \{0,1\}^{k_i}$. Here, $R_i = k_i/n$ is called the rate of the i-th write. The cells are all at level 0 before the first write [7].

3.2 Write-Once Memory Codes

This section describes binary write-once memory (WOM) codes. Note that we only deal binary two-write ($t = 2$) WOM codes in our work. WOM codes allow reusing of a WOM medium by introducing redundancy into the recorded bit sequence and, in subsequent write operations, observing the state of the memory with a new bit sequence.

Definition 3.2.1 A $(2^{nR_1}, 2^{nR_2}, n)$ two-write binary WOM code consists of two message sets $m_1 \in \{1, 2, ..., 2^{nR_1}\}$, $m_2 \in \{1, 2, ..., 2^{nR_2}\}$, and two codebooks C^1, C^2, and an alphabet $\mathcal{X}$, where $(X_1^1, X_2^1, .., X_n^1) \in C^1$, $(X_1^2, X_2^2, .., X_n^2) \in C^2$ are the WOM codebooks, and $(\mathcal{X})^n$ is a stored codeword in the write-once medium at each write.

The messages for the first write: M_1 and the second write: M_2 are chosen from the sets m_1 and m_2, respectively, then encoded into corresponding codewords by each encoding function.

The encoding function f_1 for the first write is:

$$f_1 : \{1, 2, .., 2^{nR_1}\} \rightarrow C^1.$$

The second write observes the first write codeword, giving encoding function f_2:

$$f_2 : \{1, 2, .., 2^{nR_2}\} \times C^1 \rightarrow C^2.$$

The i-th write codeword is written onto the write-once medium. When the reading of M_i happens, the decoding function g_i recovers the message M_i by:

$$g_i : (\mathcal{X}^i)^n \to \{1, 2, .., 2^{nR_i}\},$$

for $i = 1, 2$.

$R_{sum} = \sum_{i=1}^{2} R_i$ is the sum-rate of the code.

3.3 WOM codes capacity

This section describes the capacity of binary two-write WOM codes, which was given by Heegard [12].

Definition 3.3.1 The rate for $t = 2$ write $(R_1 = k_1/n, R_2 = k_2/n)$ is *achievable* if we can store a sequence of messages at these rates for some n.

Theorem 3.3.1 The capacity of two-write binary WOM codes is the closure of the convex hull of the set of all achievable rates (R_1, R_2) satisfying:

$$R_1 \leq h(p_1), \tag{3.1}$$
$$R_2 \leq (1 - p_1)h(p_2), \tag{3.2}$$

for $0 \leq p_1, p_2 \leq \frac{1}{2}$. Here, $h(\cdot)$ denotes the binary entropy function.

This *WOM input distribution* is of interest in this paper. Here, p_1 corresponds to the input distribution $p(x^1 = 1) = p_1$ for the first write, and for the second write define p_2 as:

$$p(x^2 = 1|x^1) = \begin{cases} p_2 & \text{for } x^1 = 0, \\ 1 & \text{for } x^1 = 1. \end{cases} \tag{3.3}$$

Moreover, $p(x^2 = 0|x^1 = 1) = 0$ (see Table 3.1). It is well-known that the maximum of sum-rate $R_1 + R_2$ is $\log_2 3$. To achieve this, choose $p_1 = 1/3$ and $p_2 = 1/2$.

Table 3.1 WOM input distribution

$p(x^2\|x^1)$		X^2	
		$x^2 = 0$	$x^2 = 1$
X^1	$x^1 = 0$	$1 - p_2$	p_2
	$x^1 = 1$	0	1

3.4 (3,2) WOM Codes

This section shows an example, the well-known $(n = 3, k = 2)$ WOM code that encodes two data bits $(k = 2)$ to codewords of three bits ($n = 3$ cells are needed to store codewords). The (3,2) WOM code codebooks is shown in Table 3.2. Also, Fig. 3.1 shows as Boolean 3-cube, which illustrates how 3-bit codewords are each assigned 2-bit values to represent.

Table 3.2 (3,2) WOM Code code book

Message M_i	First Write C_1 $X_1^1X_2^1X_3^1$	Second Write C_2 (if data changes $M_1 \neq M_2$) $X_1^2X_2^2X_3^2$
00	000	111
01	001	110
10	010	101
11	100	011

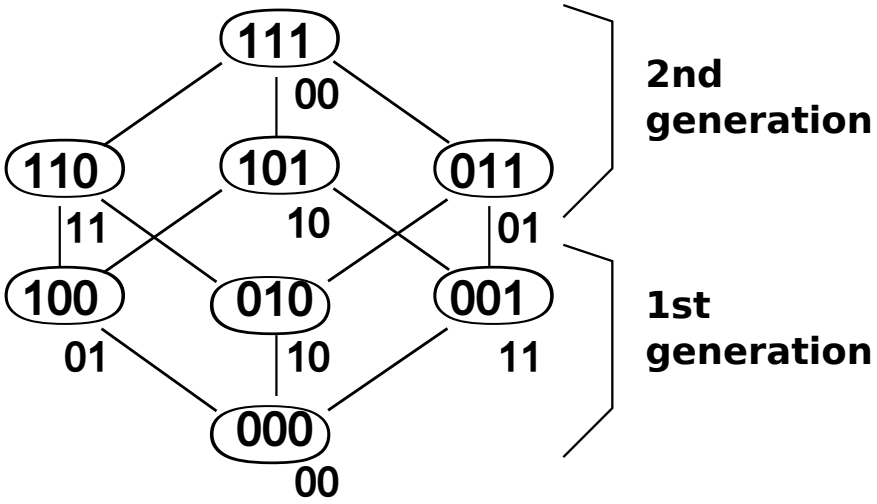

Fig. 3.1 (3,2) WOM code on the Boolean 3-cube.

It is easy to verify that after the first 2-bit data is encoded into a 3-bit codeword, if the second 2-bit data is different from the first, the 3-bit codeword into which it is encoded into does not change any code bit 1 into a code bit 0, ensuring it can be recorded in the WOM. The rate of each write $R_1 = R_2 = 2/3$.

Let us show a concrete example of data write using (3,2) WOM codes (see Fig.3.2). A pair of messages is written onto WOM at each write. At the first data write, a message $M_1 = [10]$ is encoded into $X_1^1X_2^1X_3^1 = [010]$ by the first codebook C_1, then written onto WOM. At the second write, a message $M_2 = [01]$ is encoded into $X_1^2X_2^2X_3^2 = [110]$ by the second codebook C_2, because the second write observed the state of the WOM and $M_1 \neq M_2$ in this example. This codeword [110] is overwritten onto a stored codeword [010] in the WOM cells. Note that WOM cells cannot change $1 \rightarrow 0$, i.e. WOM cells store a codeword [110] after the second write. When the reading of message M_i happens, the decoder recovers the message M_i as follows:

Lemma 3.4.1 [6] WOM codes decoding (an example in the (3,2) WOM codes case) is done: The memory word *abc* represents 2-bit value $(b \oplus c)$, $(a \oplus c)$, no matter whether the WOM has been written once or twice.

For example, when the reading of message M_1 happens after the first write, a codeword [010] is stored in the WOM. Decoder outputs the recovered message $\hat{M}_1 = [1 \oplus 0, 0 \oplus 0] = [10]$,

which is the same as the message at the first write M_1 = [10].

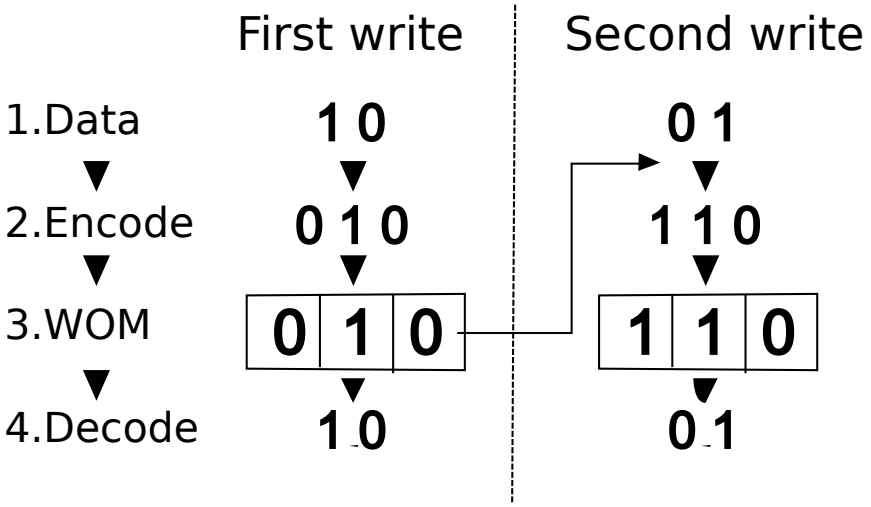

Fig. 3.2 Data write onto WOM using (3,2) WOM code.

Chapter 4

Applying WOM codes to BS-AMAC

This chapter shows how to apply coding scheme: WOM codes to the channel: BS-AMAC and their achievable rates. We also shows that WOM codes can achieve the BS-AMAC maximum sum-rate. Moreover, WOM codes specific input distribution is helpful for a BS-AMAC, is shown.

4.1 BS-AMAC using WOM Codes

This section describes how WOM codes are used for the BS-AMAC. A key property of two-write WOM codes is that the second write observes the first write codeword. For the BS-AMAC, this corresponds to User 2 knowing the codeword produced by User 1 pictured in Fig.4.1. Thus, the BS-AMAC channel is highly appropriate for the application of WOM codes.

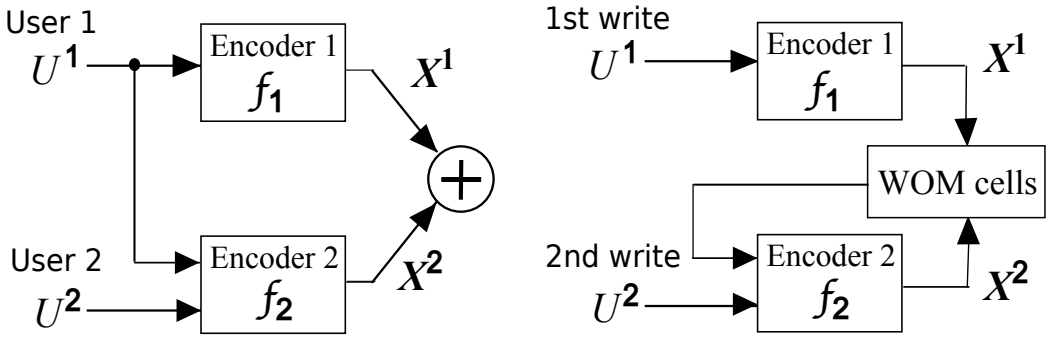

Fig. 4.1 (a) BS-AMAC (b) Data writing using WOM codes.

We assume the BS-AMAC using two-write WOM codes, implying with input distribution that follows the WOM input distribution defined at (3.3) (i.e. the input combination $(X^1, X^2) = (1, 0)$ is disallowed). Hence, we call this BS-AMAC with an input distribution (3.3) as the *WOM for AMAC*.

The rate defined for a two-write WOM code is the same as the rate for the BS-AMAC, where n represents the number of code bits as well as the number of channel uses (per user). The rates are also the same, in the BS-AMAC case, user i can transmit one of 2^{nR_i} messages, which is identical to the WOM code definition of rate.

4.2 Encoding in WOM for AMAC

This section details the system diagram, WOM for AMAC and a decoder pictured in 4.2. In the WOM for AMAC, User 1 and User 2 choose indices U^1 and U^2 uniformly from the set $u^1 \in \{1, 2, ..., 2^{nR_1}\}$ and $u^2 \in \{1, 2, ..., 2^{nR_2}\}$. The encoding function for U^1 uses the WOM codebook of the first write C_1 and outputs $f_1(U^1)$ to achieve a rate R_1:

$$f_1 : \{1, 2, .., 2^{nR_1}\} \to (\mathcal{X}^1)^n,$$

and the encoder for U^2 observes the message U^1, then uses the WOM codebook of the second write C_2 if $U^1 \neq U^2$ (and if $U^1 = U^2$, Encoder for U^2 outputs the same codeword as U^1) and outputs $f_2(U^1, U^2)$ to achieve rate R_2.

$$f_2 : \{1, 2, .., 2^{nR_2}\} \times (\mathcal{X}^1)^n \to (\mathcal{X}^2)^n.$$

A BS-AMAC channel output Y^n is the integer-valued addition of both codewords, $(X^1)^n$ and $(X^2)^n$ with no errors $P_e = 0$, or $(Y^1)^n$ and $(Y^2)^n$ with errors $P_e \neq 0$. The decoder translates Y^n into appropriate codewords $(\hat{X}^1, \hat{X}^2)$, respectively:

$$g : \mathcal{Y}^n \to (\mathcal{X}^1)^n \times (\mathcal{X}^2)^n.$$

In our research, we consider two types of decoding functions, which are described in Chap. 5.

Let us show a concrete example of WOM for AMAC using (3,2) WOM codes for error-free case $P_e = 0$. A pair of messages is transmitted over the BS-AMAC with the error probability $P_e = 0$. Suppose that User 1 and User 2 simultaneously send a message $U^1 = [10]$ and $U^2 = [01]$, respectively. The message U^1 is encoded into $X_1^1 X_2^1 X_3^1 = [010]$ by the first codebook C_1. Also, the message U^2 is encoded into $X_1^2 X_2^2 X_3^2 = [110]$ by the second codebook C_2, because $U^1 \neq U^2$ (see Table 3.2). The decoder receives a sequence $Y_1 Y_2 Y_3 = [120]$ which is the integer-valued addition of both codewords, $X_1^1 X_2^1 X_3^1$ and $X_1^2 X_2^2 X_3^2$ for error-free case $P_e = 0$, then outputs appropriate codewords by implementing decoding.

X^1	X^2	Y
0	0	0
0	1	1
1	0	1
1	1	2

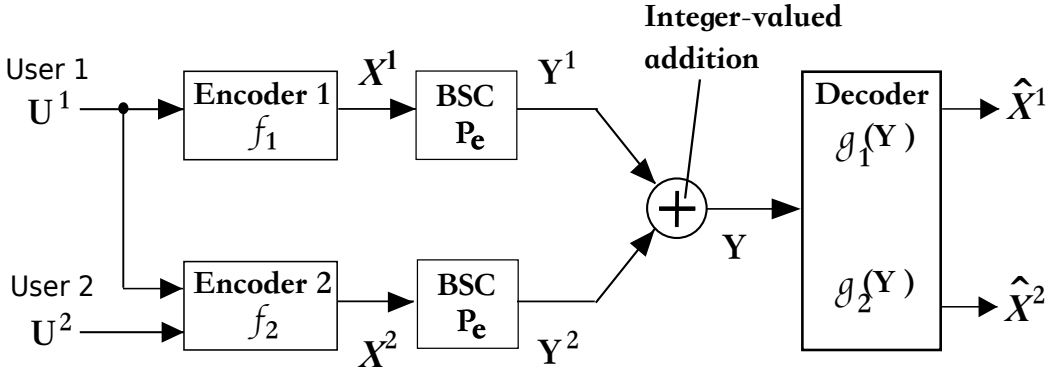

Fig. 4.2 WOM for AMAC —- system diagram.

4.3 Achievable Rates

This section compares the BS-AMAC capacity region and WOM for AMAC *achievable rate region*.

Definition 4.3.1 The achievable rate region is some subset of the closure of the convex hull of the set of all achievable rates, subject to various restrictions.

In the WOM for AMAC, the size of achievable rate region is reduced by WOM input distribution (3.3).

The next theorem shows that from a two-write binary WOM code of rate (R_1, R_2), it is possible to construct a code for a WOM for AMAC for error-free case, when $P_e = 0$.

Theorem 4.3.1 If (R_1, R_2) is an achievable rate pair for a two-write WOM code, then (R_1, R_2) is an achievable rate pair for the BS-AMAC channel for error-free case $P_e = 0$.

Proof: Assume we have a two-write WOM code with the capacity given by the inequalities (3.1) and (3.2). The inequalities (2.9) and (2.10) are:

$$R_2 \leq H(X^2|X^1) - H(X^2|X^1, Y), \tag{4.1}$$

$$R_1 + R_2 \leq H(X^1, X^2) - H(X^1, X^2|Y). \tag{4.2}$$

With the restriction to the input distribution in (3.3) and with $P_e = 0$, it is clear that $H(X^2|X^1, Y) = H(X^1, X^2|Y) = 0$.

$$\begin{aligned} R_2 &\leq H(X^2|X^1) \\ &= -\sum_{x^1,x^2} p(x^1, x^2) \log_2 p(x^2|x^1) \\ &= (1 - p_1)h(p_2), \end{aligned} \tag{4.3}$$

$$\begin{aligned} R_1 + R_2 &\leq H(X^1) + H(X^2|X^1) \\ &= -\sum_{x^1} p(x^1) \log_2 p(x^1) \\ &\quad - \sum_{x^1,x^2} p(x^1, x^2) \log_2 p(x^2|x^1) \\ &= h(p_1) + (1 - p_1)h(p_2) \end{aligned} \tag{4.4}$$

where the joint input distribution $p(x^1)p(x^2|x^1)$ is used to obtain (4.3) and (4.4), which is given by Table 4.1 for convenience.

These inequalities (4.3) and (4.4) are identical to (2.9) and (2.10), thereby an achievable rate for the two write WOM code is also an achievable rate of the BS-AMAC for error-free case. If we release the restriction on conditional input distribution $p(x^2|x^1)$ to the WOM for AMAC, then this rate region could be bigger, i.e. the converse does not hold. ■

In the study of WOM codes, the sum-rate $R_1 + R_2$ is of importance. The maximum of $R_1 + R_2$ is clearly a line which forms part of the boundary of the capacity region. The next section shows that the WOM input distribution achieves one point on the boundary of the capacity region of the BS-AMAC.

Table 4.1 Joint input distribution $p(x^1)p(x^2|x^1)$ on $\mathcal{X}^1 \times \mathcal{X}^2$

$p(x^1)p(x^2\|x^1)$		X^2		
		$x^2 = 0$	$x^2 = 1$	$p(x^1)$
X^1	$x^1 = 0$	$(1-p_1)(1-p_2)$	$(1-p_1)p_2$	$1-p_1$
	$x^1 = 1$	0	p_1	p_1
	$p(x^2)$	$(1-p_1)(1-p_2)$	$(1-p_1)p_2 + p_1$	

4.4 WOM Input Distribution Achieves BS-AMAC Capacity

Theorem 4.4.1 For the BS-AMAC model with $P_e \geq 0$, there exists a rate pair (R_1', R_2') on the boundary of the BS-AMAC capacity region, which is achieved by the WOM input distribution.

Proof: The overview of the proof is given first. The first part of the proof shows the existence of a WOM code input distribution that achieves the maximum of the sum rate $R_1' + R_2'$. This is done by assuming the existence of one input distribution which achieves the maximum of the sum rate, and this is used to show that a set of input distributions achieves the maximum. One member of this set is the WOM input distribution (3.3).

The second part of the proof simply shows how to find the pair (R_1', R_2'), and that it must be on the boundary of the BS-AMAC capacity region.

Proof: For shorthand, let $X^1X^2 = 0, 1, 2, 3$ correspond to $(X^1, X^2) = (00), (01), (10), (11)$, respectively. Let $p_i = \Pr(X^1X^2 = i)$, for $i = 0, 1, 2, 3$. The input distribution is $[p_0, p_1, p_2, p_3]$, and can be written alternatively as:

$$[p_0, \lambda p, \overline{\lambda} p, p_3], \tag{4.5}$$

where $0 \leq \lambda \leq 1$, $p = p_1 + p_2$ and $\overline{\lambda} = 1 - \lambda$.

The maximum of the sum-rate is:

$$R_1' + R_2' = \max_{p_0,\ldots,p_3} I(X^1X^2, Y). \tag{4.6}$$

Let $p_0^*, p_1^*, p_2^*, p_3^*$ be a maximizing input distribution, which clearly exists, but is not unique. This can be written alternatively written as:

$$[p_0^*, \lambda^* p^*, \overline{\lambda}^* p^*, p_3^*], \tag{4.7}$$

with $p^* = p_1^* + p_2^*$ and $\lambda^* = \frac{p_1^*}{p_1^* + p_2^*}$. Now, consider a relaxed input distribution:

$$[p_0^*, \lambda p^*, \overline{\lambda} p^*, p_3^*] \tag{4.8}$$

with arbitrary $0 \leq \lambda \leq 1$.

It is shown that the mutual information $I(X^1X^2;Y) = H(Y) - H(Y|X^1X^2)$ is independent of λ, under the relaxed input distribution (4.8). Write $H(Y|X^1X^2)$ as:

$$p_0 H(Y|X^1X^2 = 0) + p_1 H(Y|X^1X^2 = 1) + p_2 H(Y|X^1X^2 = 2) + p_3 H(Y|X^1X^2 = 3).$$

It is straightforward to show that $H(Y|X^1X^2 = 1) = H(Y|X^1X^2 = 2)$ by direct evaluation, for example:

$$\begin{aligned} H(Y|X^1X^2 = 1) = {} & P_{\mathrm{e}}(1-P_{\mathrm{e}}) \log_2 P_{\mathrm{e}}(1-P_{\mathrm{e}}) \\ & + \left((1-P_{\mathrm{e}})^2 + P_{\mathrm{e}}^2\right) \log\left((1-P_{\mathrm{e}})^2 + P_{\mathrm{e}}^2\right) \\ & + P_{\mathrm{e}}(1-P_{\mathrm{e}}) \log P_{\mathrm{e}}(1-P_{\mathrm{e}}). \end{aligned}$$

Then, $H(Y|X^1X^2)$ can be written as:

$$p_0 H(Y|X^1X^2 = 0) + (\lambda p^* + \overline{\lambda} p^*) H(Y|X^1X^2 = 1) + p_3 H(Y|X^1X^2 = 3),$$

which does not depend on λ. Similarly, it can be shown by direct evaluation that $H(Y)$ is also independent of λ, but this is tedious and is omitted.

By assumption, $I(X^1X^2;Y)$ maximized by (4.7). But because $I(X^1X^2;Y)$ is independent of λ, any value of λ with $0 \leq \lambda \leq 1$ will achieve the maximum. If we choose $\lambda = 1$, then one such maximizing input distribution is:

$$[p_0^*, p_1^* + p_2^*, 0, p_3^*], \tag{4.9}$$

which corresponds to a WOM code distribution (3.3). Thus, the WOM code input distribution achieves the maximum of the sum-rate $R_1' + R_2'$ for the BS-AMAC channel.

For the second part of the proof, recall the rate region

$$R_1 + R_2 \leq I(X^1X^2;Y) \tag{4.10}$$

$$R_2 \leq I(X^2;Y|X^1), \tag{4.11}$$

and consider the evaluation of the two mutual information terms using the relaxed input distribution (4.8). Varying λ will sweep points along the straight edge of the boundary, as in Fig. 4.3. This is because $I(X^1X^2;Y)$ is independent of λ, but $I(X^2;Y|X^1)$ depends on λ.

Now, fix $\lambda = 1$ and define R_1' and R_2' as the corresponding rates:

$$R_2' = I(X^2;Y|X^1) \tag{4.12}$$

$$R_1' = I(X^1X^2;Y) - R_2^*, \tag{4.13}$$

that is both mutual information terms are evaluated with input distribution (4.9). The WOM code input distribution achieves the maximum of the sum rates, corresponding to the straight line boundary of the capacity region. But, the WOM code input distribution achieves one rate pair on the boundary, which is given by (R_1', R_2'), as shown above. ■

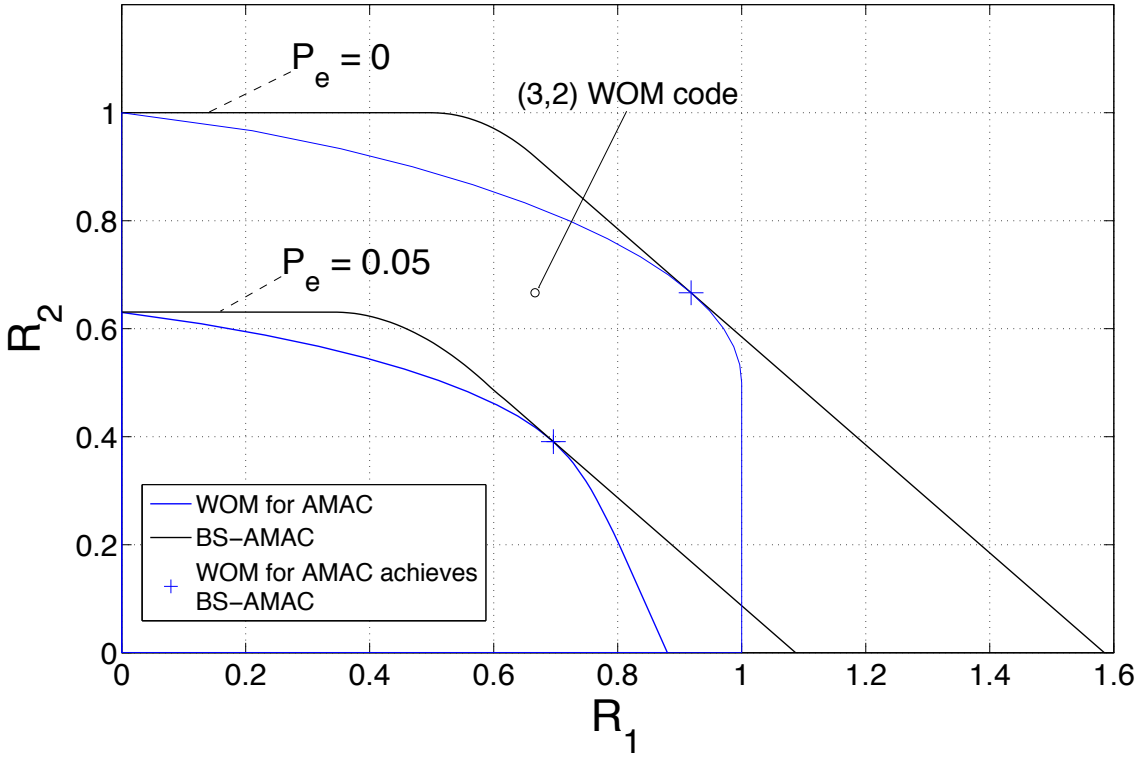

Fig. 4.3 Capacity region of the BS-AMAC and achievable rate region of the WOM for AMAC.

The capacity regions for the BS-AMAC (without restrictions) and achievable rates of the WOM for AMAC (with the WOM code restriction) for $P_e = 0$ and 0.05 are plotted in Fig.4.3, where the regions touch at one point ($(R_1, R_2) = (h(1/3), 2/3)$ and $(R_1, R_2) \approx (0.6923, 0.3928)$, respectively) achieving maximum sum-rate.

Here, an achievable rate of the WOM for AMAC system is a rate pair such that the probability of decoding error goes to 0 (as in Sec.2.1), subject to the restriction (3.3).

4.4.1 Input Distribution Search

This section shows that a non-uniform input distribution is helpful for a BS-AMAC. Linear binary codes are often used in cooperative wireless communications, however linear binary codes have uniform input distribution. On the BS-AMAC, the two users interfere with each other, thereby we have to find a suitable joint input distribution $p(x^1)p(x^2|x^1)$ to achieve the BS-AMAC capacity.

The capacity region of the BS-AMAC was found by an exhaustive search over p_1, p_2 and α (See Table 2.2) to find the convex hull. The WOM codes capacity region was done likewise with WOM input distribution (3.3), since an achievable rate pair for the two-write binary WOM codes is an achievable rate pair for the WOM for AMAC, for the error-free case (See proof of Theorem 4.1). If we fix $p_1 = p_2 = 1/2$ and vary α, a region is found, which corresponds to the linear binary codes achievable rates on the BS-AMAC. These three

regions are shown in Fig. 4.4.

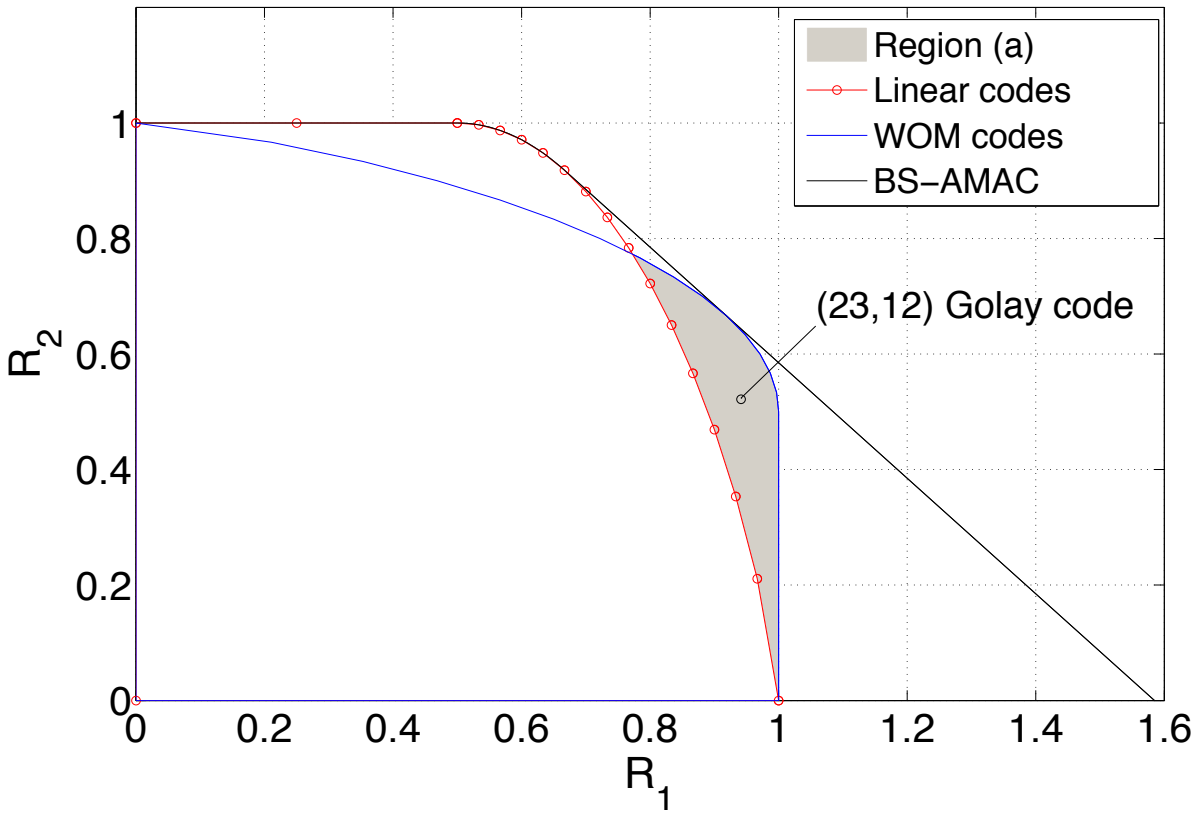

Fig. 4.4 Input distribution search.

In Fig. 4.4, Region (a) represent rate pairs that are not achievable using linear binary codes, but are achievable using WOM codes. The two-write WOM code based on $n = 23$ Golay code given by Yaakobi et al. [11] has rate pair $(R_1, R_2) = (0.9415, 0.5217)$, which is also shown. This illustrates that non-uniform input distributions, such as WOM codes described in this paper, are helpful for achieving capacity.

Chapter 5

Decoding scheme

Applying WOM codes to the BS-AMAC provides efficienct separation of the two codewords at the receiver, without using joint iterative decoding or successive interference cancellation. In our scheme, we have two types of low-complexity decoding: (1) Hard decision decoding: decomposed system using symbol-wise estimation and (2) Soft decision decoding: a posteriori probability (APP) decoder.

5.1 Decomposed System

This section describes the *decomposed system* pictured in Fig. 5.1.

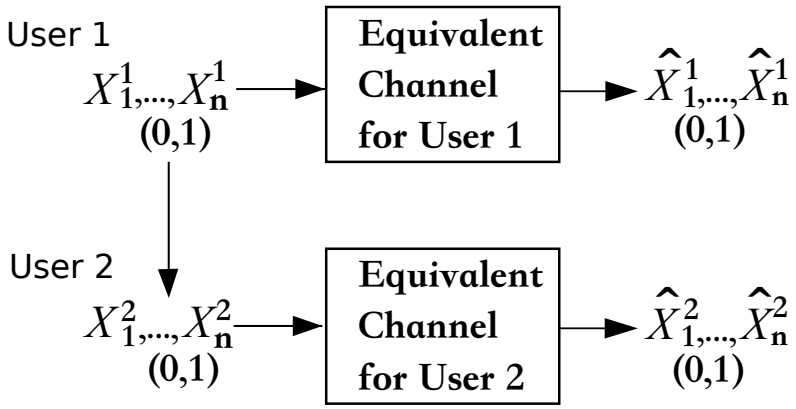

Fig. 5.1 Decomposed system.

The decomposed system consists of four alphabets $\mathcal{X}^1, \mathcal{X}^2$, and $\hat{\mathcal{X}}^1, \hat{\mathcal{X}}^2$ where $X^1 \in \mathcal{X}^1$ and $X^2 \in \mathcal{X}^2$ are input symbols, and $\hat{X} \in \hat{\mathcal{X}}^1$ and $\hat{X}^2 \in \hat{\mathcal{X}}^2$ are estimated symbols respectively. The decomposed system consists of two parts, BS-AMAC $(X^1, X^2) \rightarrow Y$ with the WOM input distribution (3.3), and two estimation functions $Y \rightarrow g_1(Y)$ and $g_2(Y) \rightarrow \hat{X}^1$ and $\hat{X}^2$.

We describe the idea of a hard decision decoding: *symbol-wise estimation* for channel output Y in the decomposed system. The estimation is performed symbol-by-symbol to decompose the received sequence $Y_1, Y_2, ..., Y_n$ into two data streams $\hat{X}^1_1, \hat{X}^1_2, ..., \hat{X}^1_n$ and $\hat{X}^2_1, \hat{X}^2_2, ..., \hat{X}^2_n$ using decoding functions g_i:

$$g_1 : \mathcal{Y} \rightarrow \hat{\mathcal{X}}^1, \text{and}$$

$$g_2 : \mathcal{Y} \to \hat{\mathcal{X}}^2,$$

for User 1 and User 2 respectively. For the WOM for AMAC, each decoding function outputs:

$$g_1(Y) = \begin{cases} 0 & if\ y = 0, 1, \\ 1 & if\ y = 2, \end{cases} \tag{5.1}$$

$$g_2(Y) = \begin{cases} 0 & if\ y = 0, \\ 1 & if\ y = 1, 2. \end{cases} \tag{5.2}$$

for User 1 and User 2 respectively, so that $\hat{X}^1 = g_1(Y)$ and $\hat{X}^2 = g_2(Y)$. Estimation is pictured in Fig. 5.2. In the error-free $P_e = 0$ case, symbol-wise estimation introduces no errors, shown as follows. When $Y = 0$ or $Y = 2$, the decoder estimate should clearly be $(\hat{X}^1, \hat{X}^2) = (0, 0)$ and $(\hat{X}^1, \hat{X}^2) = (1, 1)$, respectively. When $Y = 1$, there is also no ambiguity, and the decoder outputs $(\hat{X}^1, \hat{X}^2) = (0, 1)$ because the combination $(X^1, X^2) = (1, 0)$ is disallowed in the WOM input distribution. In the decomposed system, the WOM for AMAC system (i.e. two user's codewords are correlated) is equivalent to two separated, or two decomposed channels, while maintaining the correlation.

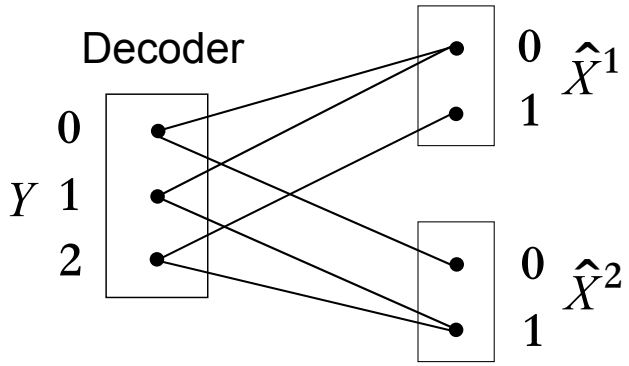

Fig. 5.2 Symbol-wise estimation for decomposed system.

5.2 Achievable Rates for Decomposed System

Next, we study the decomposed system achievable rates when $P_e \geq 0$. The decomposed system uses the WOM input distribution (3.3), which reduces the achievable rate region, however the restriction induces a property useful for decoding.

The next corollary shows inequalities for an achievable rate of the decomposed system.

Corollary 5.2.1 Any rate pair (R_1, R_2) satisfying:

$$R_2 \leq I(X^2; \hat{X}^2 | X^1) \tag{5.3}$$

$$R_1 + R_2 \leq I(X^1, X^2; \hat{X}^1, \hat{X}^2) \tag{5.4}$$

is an achievable rate pair for the decomposed system subject to the restrictions the WOM input distribution (3.3) and the symbol-wise estimation.

Proof: The proof assumes a WOM input distribution (3.3) and the decomposed system is using symbol-wise estimation g_1 and g_2 given by (5.1) and (5.2). Observe that $(X^1, X^2) \to Y \to (\hat{X}^1, \hat{X}^2)$ forms a Markov chain, and this is applied to the restriction of the AMAC capacity region (2.9) and (2.10). Since $\hat{X}^1 = g_1(Y)$ and $\hat{X}^2 = g_2(Y)$, by the data processing inequality in Sec.1.2.4, $I(X^2; \hat{X}^2|X^1) \leq I(X^2; Y|X^1)$ and $I(X^1, X^2; \hat{X}^1, \hat{X}^2) \leq I(X^1, X^2; Y)$. Thus, the decomposed system achievable rates inequalities (5.3) and (5.4) are obtained. ■

The decomposed system achievable rate region is the closure of the convex hull of the set of all achievable rates (R_1, R_2) satisfying (5.3) and (5.4).

The decomposed system achievable rate region (5.3) and (5.4), are compared to the WOM for AMAC achievable rates (2.9) and (2.10), which are pictured in Fig. 5.3. Both regions are the same for the error-free case, however the decomposed system achievable rate region is never larger than the WOM for AMAC region when $P_e > 0$, nonetheless, the achievable rate region is large and have some practical significance. Accordingly, we study the gaps between achievable rates of the WOM for AMAC and the decomposed system.

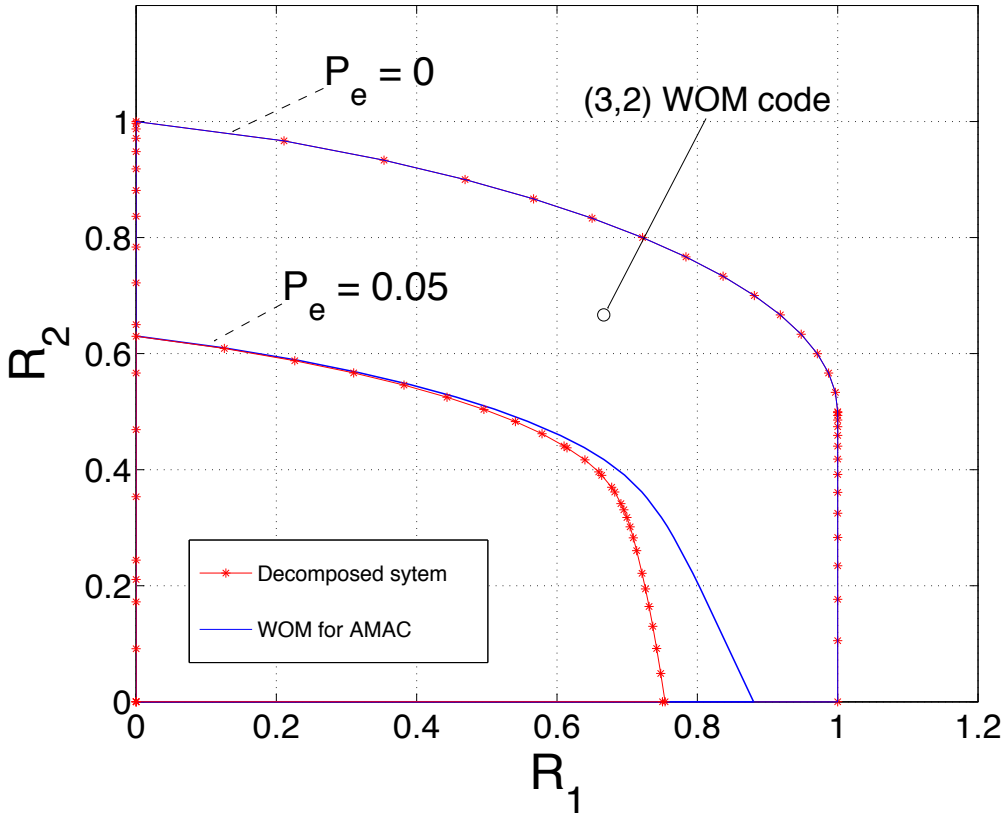

Fig. 5.3 Achievable rates of the WOM for AMAC and decomposed system.

We compute two types of gaps. 1) The gap in maximum sum-rate, maximum sum-rate for the WOM for AMAC is $\max I(X^1, X^2; Y)$, and for the decomposed system is $\max I(X^1, X^2; \hat{X}^1, \hat{X}^2)$. 2) The gap of achievable rates $R_1 + R_2$ when $R_1 = R_2$. This second

case is of practical interest, for example in block-Markov relaying. Both gaps are pictured in Fig. 5.4, which shows that the achievable rates of decomposed system is always smaller or equal to the WOM for AMAC.

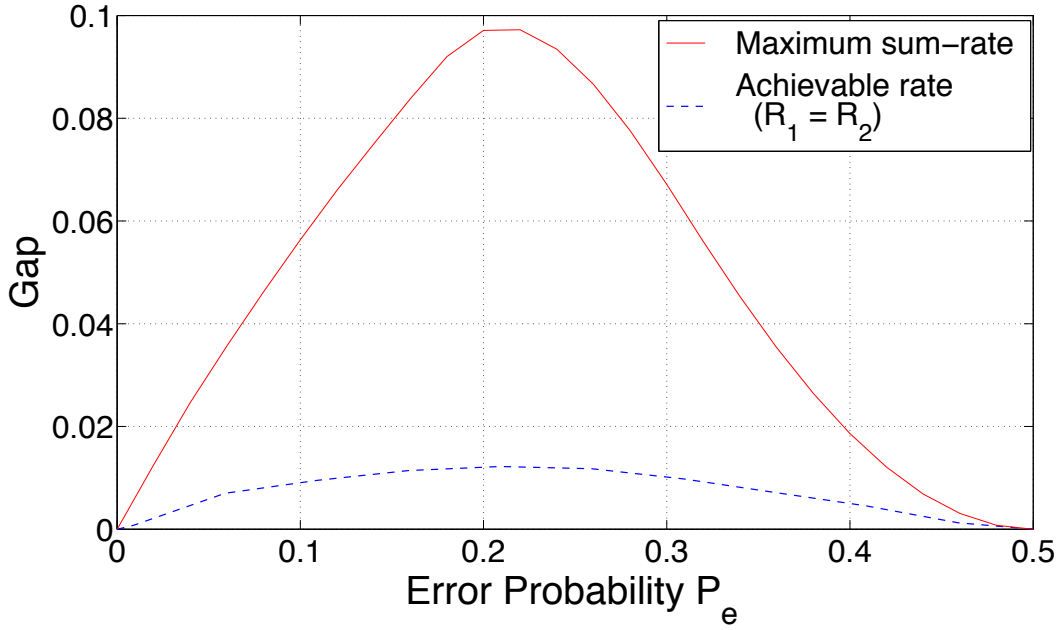

Fig. 5.4 Gap of two achievable rates for WOM for AMAC and Decomposed system.

5.3 APP Decoder

This section shows a soft decision decoding: APP decoding, of WOM codes for the BS-AMAC. For APP decoding, mutual information is evaluated, and gives the highest information rate that a capacity-approaching code could achieve. Note that we use codeword sequences denoted by $\mathbf{X} = (X_1, X_2, ..., X_n)$ in this section.

Definition 5.3.1 *APP is the probability of $U = u$ given the observation $\mathbf{Y}$, that is:*

$$p(U^i|\mathbf{Y} = \mathbf{y}) = \frac{p(\mathbf{Y}|U^i = u)P(U^i)}{p(\mathbf{Y})} = \frac{p(U^i, \mathbf{Y})}{p(\mathbf{Y})}. \tag{5.5}$$

Begin by writing the joint distribution $p(\mathbf{Y}|U^i)P(U^i)$ as:

$$p(U^i, \mathbf{Y}) = \sum_{\mathbf{X}^1\mathbf{X}^2 \in C_1, C_2} p(U^i, \mathbf{Y}, \mathbf{X}^1, \mathbf{X}^2)$$

$$= \sum_{\mathbf{X}^1\mathbf{X}^2} p(U^i|\mathbf{X}^1\mathbf{X}^2)p(\mathbf{Y}|\mathbf{X}^1\mathbf{X}^2)p(\mathbf{X}^2|\mathbf{X}^1)p(\mathbf{X}^1) \tag{5.6}$$

Encoder 1 chooses a codeword $\mathbf{X}^1$ from codebook C_1 with uniform probability distribution, so $p(\mathbf{X}^1) = \frac{1}{2^{nR_1}}$. We call attention to a particular special case. In WOM codes, if $u^1 = u^2$, then the state of the memory does not need to be changed.

That is $C_1 \subset C_2$ and $\mathbf{X}^2 \in C_1$ is possible. While codewords for $\mathbf{X}^1$ are uniformly distributed on C_1, codewords for $\mathbf{X}^2$ are not uniformly distributed on C_2.

The channel is characterized by $p(\mathbf{Y}|\mathbf{X}^1\mathbf{X}^2)$ which depends on P_e. $p(\mathbf{X}^2|\mathbf{X}^1)$ is obtained from the WOM-code distribution between first and second write codewords, and can be obtained from f_2. And, $p(U^1 = u^1|\mathbf{X}^1 = \mathbf{x}^1) = 1$ if $f_1(u^1) = \mathbf{x}^1$, otherwise it is zero. And $p(U^2 = u^2|\mathbf{X}^1\mathbf{X}^2 = \mathbf{x}^1\mathbf{x}^2) = 1$ if $f_2(u^2, \mathbf{x}^1) = \mathbf{x}^2$, otherwise it is zero.

The two outputs of the APP decoder are $p(U^1 = u|\mathbf{Y})$ and $p(U^2 = u|\mathbf{Y})$ computed as above.

5.3.1 Mutual Information $I(U^i; \mathbf{W}^i)$

Define new symbols $\mathbf{W}^1$ and $\mathbf{W}^2$ as the output of the decoder which is a vector of probabilities indexed by u,

$$\mathbf{W}^i = p(U^i = u|\mathbf{Y} = \mathbf{y}) \tag{5.7}$$

which could represent the message passed to an LDPC decoder. Here we deal with word probabilities in the probability domain; if bit probabilities w are computed, these can be converted to the log-likelihood ratio domain using $g(w) = \log \frac{w}{1-w}$.

The APP decoder can also be used to decompose the received sequence $\mathbf{Y}$ into two streams $\mathbf{W}^1$ and $\mathbf{W}^2$, one for each user. In this case, a short WOM code is assumed, and achievable rates for a decomposed system are characterized using mutual information, $\frac{1}{n}I(U^1; \mathbf{W}^1)$ and $\frac{1}{n}I(U^2; \mathbf{W}^2)$. For example, an LDPC code that can communicate reliably at rate R_1 can also be used for reliable communications on this WOM-coded AMAC channel, if $R_1 \leq \frac{1}{n}I(U^1; \mathbf{W})$.

For this discrete system, the set values $\mathcal{Y}^n$ is finite, and the set of decoder outputs $\mathcal{W}^i$ is similarly finite. We have $2^{nR_i} + 1 \leq |\mathcal{W}^i| \leq |\mathcal{Y}^n|$ distinct values of $\mathbf{W}$ for user i.

The set $\mathcal{W}^i$ is known, so the probability distribution $p(\mathbf{W}^i)$ is readily obtained. By numerical evaluation we obtain the probability $p(\mathbf{W}^i|U^i)$. Then it is straightforward to obtain the mutual information between the user information U^i and the symbol $\mathbf{W}^i$ given by:

$$I(U^i; \mathbf{W}^i) = \sum_{\mathcal{W}^i} \sum_{\mathcal{U}^i} p(\mathbf{W}^i, U^i) \log_2 \frac{p(\mathbf{W}^i|U^i)}{p(W^i)}. \tag{5.8}$$

5.3.2 Numerical Results for APP decoding

The effectiveness of our system is established through numerical evaluation of mutual information $I(U^i, \mathbf{W}^i)$ for the (3,2) WOM code, which has $(R_1, R_2) = (\frac{2}{3}, \frac{2}{3})$, for various values of P_e, shown in Fig. 5.5. We consider the mutual information for each user separately to obtain $I(U^1; \mathbf{W}^1)$ and $I(U^2; \mathbf{W}^2)$.

The (3,2) WOM code has sum rate $\frac{4}{3}$. By using this code, we obtained the same sum rate for $P_e = 0$. The gap between the maximum sum rate of the AMAC (assuming inifinite-length codes) and the APP decoder sum rate $I(U^1; \mathbf{W}^1) + I(U^2; \mathbf{W}^2)$ (assuming the (3,2) WOM code) is shown using a dashed line in Fig. 5.5. For the error-free case, the gap is $\log_2 3 - \frac{4}{3} = 0.2516$. Thus, even in the presence of errors, this gap is decreasing as P_e

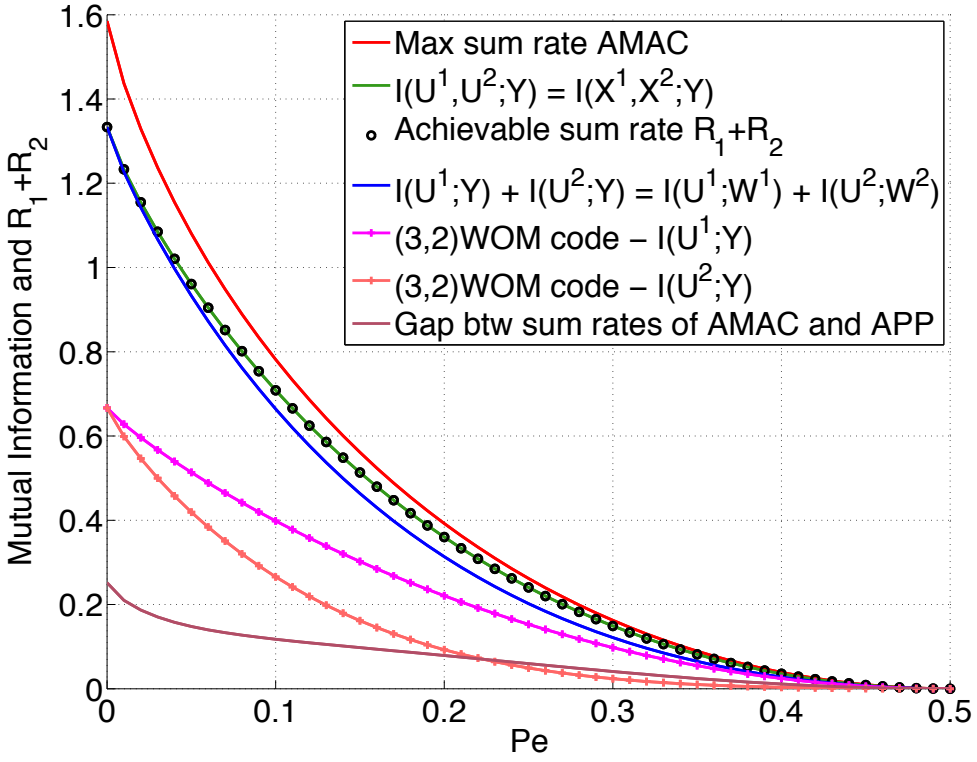

Fig. 5.5 Max sum rate of AMAC using solid-triangle line. $I(U^1, U^2; \mathbf{Y})$ and $I(\mathbf{X}^1, \mathbf{X}^2; \mathbf{Y})$ using solid line and at the same space, achievable sum rate $R_1 + R_2$ using circles. Sum of individual mutual information $I(U^1; \mathbf{Y}) + I(U^2; \mathbf{Y})$ and $I(U^1; \mathbf{W}^1) + I(U^2; \mathbf{W}^2)$ using solid lines. $I(U^1; \mathbf{Y})$ for user 1 using solid-square line and $I(U^2; \mathbf{Y})$ for user 2 using solid-cross line. Gap between the max sum rate of AMAC and APP sum rate $I(U^1; \mathbf{W}^1) + I(U^2; \mathbf{W}^2)$ in dash line. All of them using using (3,2) WOM codes excluding max sum rate of the AMAC.

increases, meaning that WOM codes are effective and can be used in the presence of noise in the channel.

The sum of mutual information for the APP decoder, $I(U^1; \mathbf{W}^1) + I(U^2; \mathbf{W}^2)$ is upper bounded by the sum $I(U^1; \mathbf{Y}) + I(U^2; \mathbf{Y})$, which is shown for reference. The restricted BS-AMAC sum rate $I(U^1, \mathbf{Y}) + I(U^2, \mathbf{Y})$ is compared with the the joint rate $I(\mathbf{X}^1, \mathbf{X}^2; Y)$ and is also pictured in Fig. 5.5, given by:

$$\frac{1}{3} I(U^1; \mathbf{Y}) + \frac{1}{3} I(U^2; \mathbf{Y}) \leq \frac{1}{3} I(\mathbf{X}^1, \mathbf{X}^2; \mathbf{Y}), \text{ and} \tag{5.9}$$

$$\frac{1}{3} I(\mathbf{X}^1, \mathbf{X}^2; \mathbf{Y}) \leq R_1 + R_2 \tag{5.10}$$

where the achievable sum rate $R_1 + R_2$ is obtained by (4.4).

Chapter 6

System Performance

Applying WOM codes to the BS-AMAC leads to low-complexity decoding. In order to build a reliable communication system, the BS-AMAC capacity-approaching error correcting codes such as low-density parity check (LDPC) codes are needed. In this chapter, we show a numerical result applying LDPC codes to the our system.

6.1 LDPC codes

This section describes an error correcting code used in our work "LDPC codes". For more details on LDPC codes, refer to Gallager et al [15], [16].

6.1.1 Introduction to LDPC codes

LDPC codes were first proposed by Robert Gallager in 1960 [15], which is a class of linear codes whose parity-check matrix $\mathbf{H}$ is sparse, i.e. the matrix contains only a small number of 1s per row or column. He also proposed an efficient iterative decoding scheme called iterative *message passing* decoding for the case of the parity-check matrix $\mathbf{H}$ is sparse.

Definition 6.1.1 A linear code of length n and dimension k is a linear subspace C with the vector space $\mathbb{F}_q^n$, where $\mathbb{F}_q^n$ denotes the finite field with q elements.

In our work, we mainly use a binary (n, k) LDPC codes, which is a binary ($q = 2$) linear block code with a parity-check matrix $\mathbf{H}$ that has a low density 1s. A parity-check matrix $\mathbf{H}$ is a $m \times n$ matrix, where $m = n - k$.

We show a parity-check matrix $\mathbf{H}$ of the $(10, 5)$ LDPC code as an example:

$$\mathbf{H} = \begin{pmatrix} 1 & 1 & 1 & 1 & 0 & 0 & 0 & 0 & 0 & 0 \\ 1 & 0 & 0 & 0 & 1 & 1 & 1 & 0 & 0 & 0 \\ 0 & 1 & 0 & 0 & 1 & 0 & 0 & 1 & 1 & 0 \\ 0 & 0 & 1 & 0 & 0 & 1 & 0 & 1 & 0 & 1 \\ 0 & 0 & 0 & 1 & 0 & 0 & 1 & 0 & 1 & 1 \end{pmatrix}. \tag{6.1}$$

Encoding of LDPC codes is done by the generator matrix $\mathbf{G}$, a $k \times n$ matrix, which maps an information vector $\mathbf{u} \in \mathbb{F}_2^k$ into codewords $\mathbf{x} \in \mathbb{F}_2^n$ as follows:

$$\mathbf{x} = \mathbf{u}\mathbf{G}.$$

For any generator matrix $\mathbf{G}$ and parity-check matrix $\mathbf{H}$ the following holds:

$$\mathbf{H}\mathbf{G}^{\mathrm{T}} = 0.$$

6.1.2 LDPC Codes Based on Sparse Graphs

LDPC codes are defined in terms of a sparse bipartite graph, called *Tanner graph*. This graph has two types of nodes, the *bit nodes* and *check nodes*. Every bit node (or check node) corresponds to a column (or row) of the parity-check matrix $\mathbf{H}$. In addition, 1s in the parity-check matrix $\mathbf{H}$ corresponds to the edges between two nodes. Two nodes connected by an edge are called *neighboring nodes*.

For simplicity, we denote the i-th bit node by b_i, $i \in \mathcal{I} = \{1, ..., n\}$, and the j-th check nodes by c_j, $j \in \mathcal{J} = \{1, ..., m\}$, where indices $\mathcal{J}$ and $\mathcal{I}$ corresponding each row and column of the parity-check matrix $\mathbf{H}$, respectively. In addition, we also represent the index set of neighboring bit nodes of check node $j \in \mathcal{J}$ by $\mathcal{N}_j = \{i \in \mathcal{I} : H_{ij} = 1\}$, and the index set of neighboring check nodes of bit node $i \in \mathcal{I}$ by $\mathcal{N}_i = \{j \in \mathcal{J} : H_{ij} = 1\}$ [17].

The Tanner graph of the (10,5) LDPC code parity-check matrix $\mathbf{H}$ described in (6.1), which is pictured in Fig.6.1. In this Tanner graph, bit node $b_i, i \in \{1, ..., 10\}$ is connected to check node c_j, $j \in \{1, ..., 5\}$ via an edge when $H_{ij} = 1$. For example, the check node c_1 is connected the bit nodes v_1, v_2, v_3, v_4, i.e. it has four neighboring bit nodes and $\mathcal{N}_j = \{1, 2, 3, 4\}$.

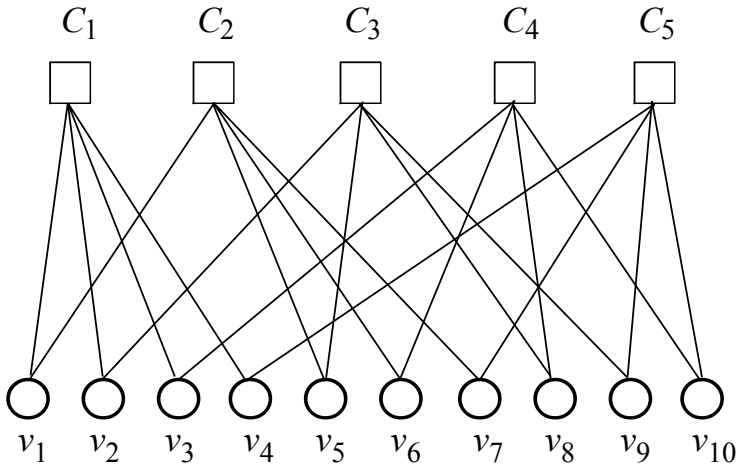

Fig. 6.1 A Tanner graph of the $(10, 5)$ LDPC code.

6.1.3 Decoding Scheme for LDPC codes

Let us consider the decoding scheme of LDPC codes called iterative *message-passing* (MP) decoding. The key property of iterative MP decoding is that the decoder gets the log-likelihood ratios (LLRs) of all received codeword symbols, then all nodes update these messages based on the messages received from the neighboring nodes in the Tanner graph.

Definition 6.1.2 The LLR in the l-th channel output symbol L_l, is defined as:

$$L_l = \log \frac{p(y_l|x_l = 0)}{p(y_l|x_l = 1)}, \tag{6.2}$$

where x_l and y_l denote the l-th encoded bit and received bit, respectively.

The iterative MP decoder consists two phases, bit node to check node $B \rightarrow C$ phase, where bit nodes send messages to check nodes along their connected edges, and check node to bit node $C \rightarrow B$ phase, where check nodes send messages to the connected bit nodes. The decoding process as follows: (1) At the first step of the decoding, bit node b_i sends a message about an LLR: L_l information to the all neighboring check nodes in $\mathcal{N}_i$. (2) In the $C \rightarrow B$ message update step in the t-th iteration, check node c_j generates an updated $C \rightarrow B$ message: $L_t[c_j \rightarrow b_i]$ using incoming messages from all connected bit nodes, then sends this information to the bit node b_i in $\mathcal{N}_j$. (3) In the $B \rightarrow C$ message update step in the t-th iteration, bit node b_i receives this updated LLR information from the neighboring check nodes. For each bit node, it generates an updated $B \rightarrow C$ message: $L_t[b_i \rightarrow c_j]$, and sends this to each connected check node c_j.

After an arbitrary number of iterations with processes (2) and (3), bit node b_i takes sum of all of the incoming LLR messages to estimate appropriate code bit i [17].

6.1.4 Sum-Product Algoritm

This section introduces an example of the iterative MP decoding algorithm, called the *sum-product* algorithm. Decoding using sum-product algorithm is also implemented as described in Sec.6.1.3.

The update rule of each step is defined as follows:

Definition 6.1.3 [16] The update rule of bit node to check node $B \rightarrow C$ is given by:

$$L_t[b_i \rightarrow c_j] = L_l + \sum_{j' \in \mathcal{N}_i \setminus j} L_{t-1}[c_{j'} \rightarrow b_i]. \tag{6.3}$$

Note that $L_{t=1}[b_i \rightarrow c_j]$ at the first iteration is equal to L_l.

Definition 6.1.4 [16] The update rule of check node to bit node $C \rightarrow B$ is given by:

$$L_t[c_j \rightarrow b_i] = \Big[\prod_{i' \in \mathcal{N}_j \setminus i} \mathrm{sign}(L_{t-1}[b_{i'} \rightarrow c_j]) \Big] \cdot \min_{i' \in \mathcal{N}_j \setminus i} |L_{t-1}[b_{i'} \rightarrow c_j]|. \tag{6.4}$$

6.2 System Model using LDPC codes

The system model using LDPC codes is pictured in Fig.6.2. There are two encoding steps: LDPC codes and WOM code, and two decoder: APP decoder and LDPC decoder. The reason why we apply the APP decoder is described below.

The system flow is straightforward as follows: (1) Both user messages U^1 and U^2 are first encoded into corresponding LDPC codewords, then applied WOM codes encoding described in Chap 4.4.1 and sent, respectively. In the above chapters, both user's codewords X^1 and

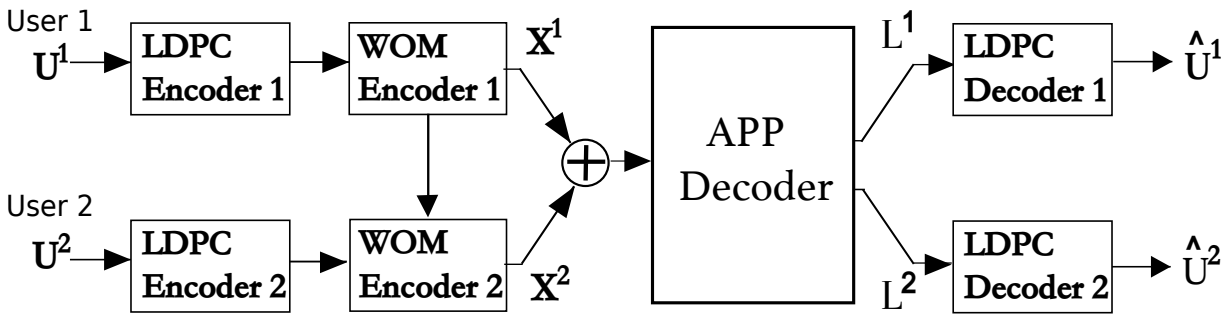

Fig. 6.2 System diagram using LDPC codes.

X^2 pass through a BSC with a common error probability P_e. However, in this section, each user's codewords passes through a BSC with error probability defined under the assumption,

$$P_{e,i} = p(Y^i \neq X^i) \; for \; i = 1, 2.$$

This is because, we hope that both user have the same bit error rate (BER) performance described in the next section. However, X^2 includes the information of X^1 and helps the communication for User 1 in the BS-AMAC, i.e. BER performance of User 2 is worse than User 1's performance with the same BSC error probability P_e. Hence, we set unique BSC error probability $P_{e,1}$ and $P_{e,2}$, respectively. (2) The APP decoder receives a sequence Y^n which is the integer-valued addition of outputs from the BSCs with error probabilities $P_{e,1}$ and $P_{e,2}$. (3) The APP decoder outputs each user's LLR L^i in order to perform the LDPC decoding described in Sec.6.1.3.

Definition 6.2.1 The LLR of i-th user: L^i in our work, is given by:

$$L^i = \log \frac{P(u^i = 0|\mathbf{Y} = \mathbf{y})}{P(u^i = 1|\mathbf{Y} = \mathbf{y})}, for \; i = 1, 2, \tag{6.5}$$

where a probability transition matrix $p(u^i|\mathbf{Y} = \mathbf{y})$ is given by (5.5).

(4) Each LDPC decoder estimates appropriate user's message $\hat{U}^1$ and $\hat{U}^2$ using LLR L^1 and L^2, respectively.

6.3 Numerical Results for Bit Error Rate

This section shows BER in our system using LDPC codes.

Definition 6.3.1 A BER is the rate at which errors occur in a transmission system:

$$\text{BER} = \frac{\text{Number of errors : } U \neq \hat{U}}{\text{Total number of bits sent}}.$$

In this numerical result, we apply (3,2) WOM codes and the well-known digital video broadcasting-satellite-second generation (DVB-S.2) LDPC codes (see Sec.3.4 and [18]). Both users communicate with rates $R_1 = R_2 = 1/3$, because of applying (3,2) WOM codes and rate $1/2$ LDPC codes (i.e. $R_{total} = R_{WOM} \times R_{LDPC} = 2/3 \times 1/2 = 1/3$). Table 6.1 shows

a parameter of the DVB-S.2 LDPC code used in our work. This LDPC code adopts the iterative MP decoding with sum-product algorithm at decoding part.

Table 6.1 Parameter of DVB-S.2 LDPC code used in our research

Date length:k	$32,400$
Block length:n	$64,800$
Transmitted frames	100
Rate	$1/2$
Decoding Algorithm	sum-product algorithm
Iterations t	50 times

A BER performance of the our system using LDPC is pictured in Fig.6.3, where the horizontal axes are error rate for User 1 as bottom and User 2 as top. Also, a parameter of a DVS-S.2 LDPC code used in our work is given in Table.6.1. Both users achieve BER below 10^{-6}, regarding *reliable* in wireless communications, when $(P = e, 1, P_{e,2}) = (0.1320, 0.0120)$. The numerical value of BSC error probability for User 1: $P_{e,1}$ was higher than $P_{e,2}$ when they achieve BER below 10^{-6}, because User 2 codeword X^2 includes User 1 information.

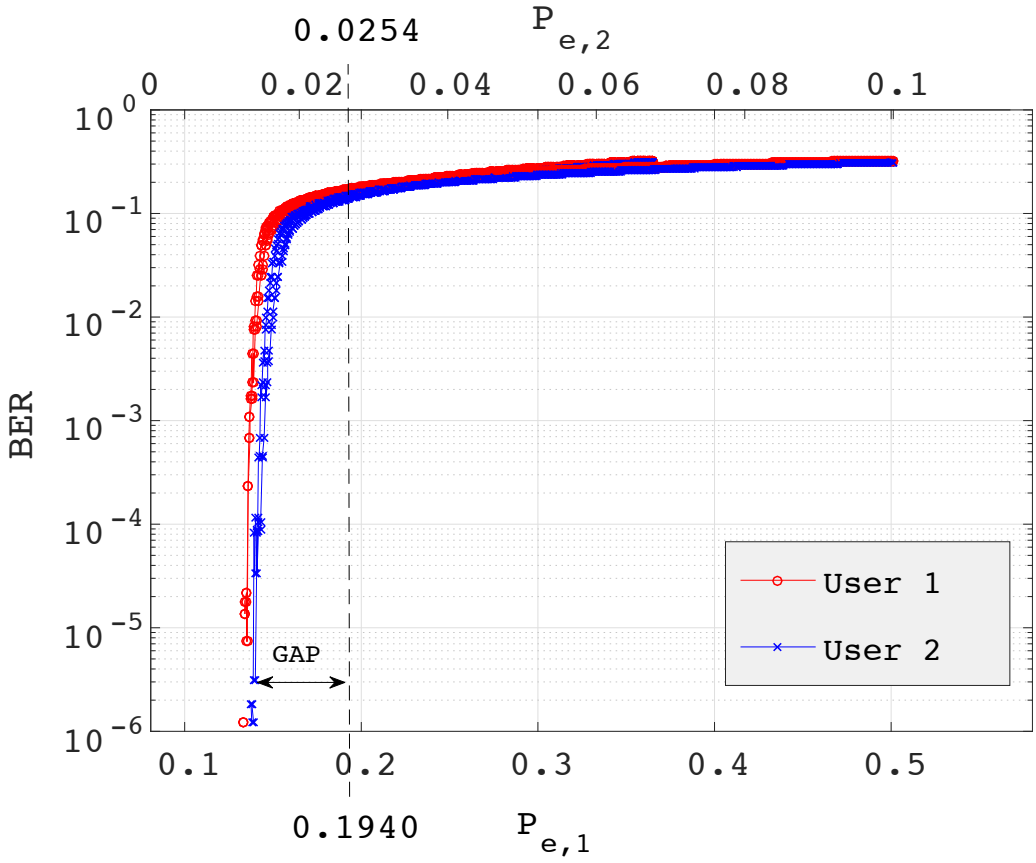

Fig. 6.3 BER of our system using LDPC codes.

There is a small gap in error probabilities $(P_{e,1}, P_{e,2})$ between an our numerical result $(P_{e,1}, P_{e,2}) = (0.1320, 0.012)$ and the theoretical value $(P_{e,1}, P_{e,2}) = (0.1940, 0.0254)$ given as follows:

Fig.6.4 shows the pairs of $(P_{e,1},\ P_{e,2})$ such that $I(U^1; \mathbf{Y}) = I(U^2; \mathbf{Y})$. Also, shown is $I(U^1; \mathbf{Y}) = I(U^2; \mathbf{Y}) = 1/3$. We want to find the channel values for which the code rate is close to the capacity. When $(P_{e,1}, P_{e,2}) = (0.1940, 0.0254)$ at a point E in Fig.6.4, the mutual informations $I(U^i; \mathbf{Y}) = 1/3$, corresponding to both user's rates $R_1 = R_2 = 1/3$. Thus, both user can simultaneously achieve BER below 10^{-6} at $(P_{e,1}, P_{e,2}) = (0.1940, 0.0254)$.

As a result, the gap in Fig.6.3 means that the error correcting code used in our research cannot approach the BS-AMAC capacity.

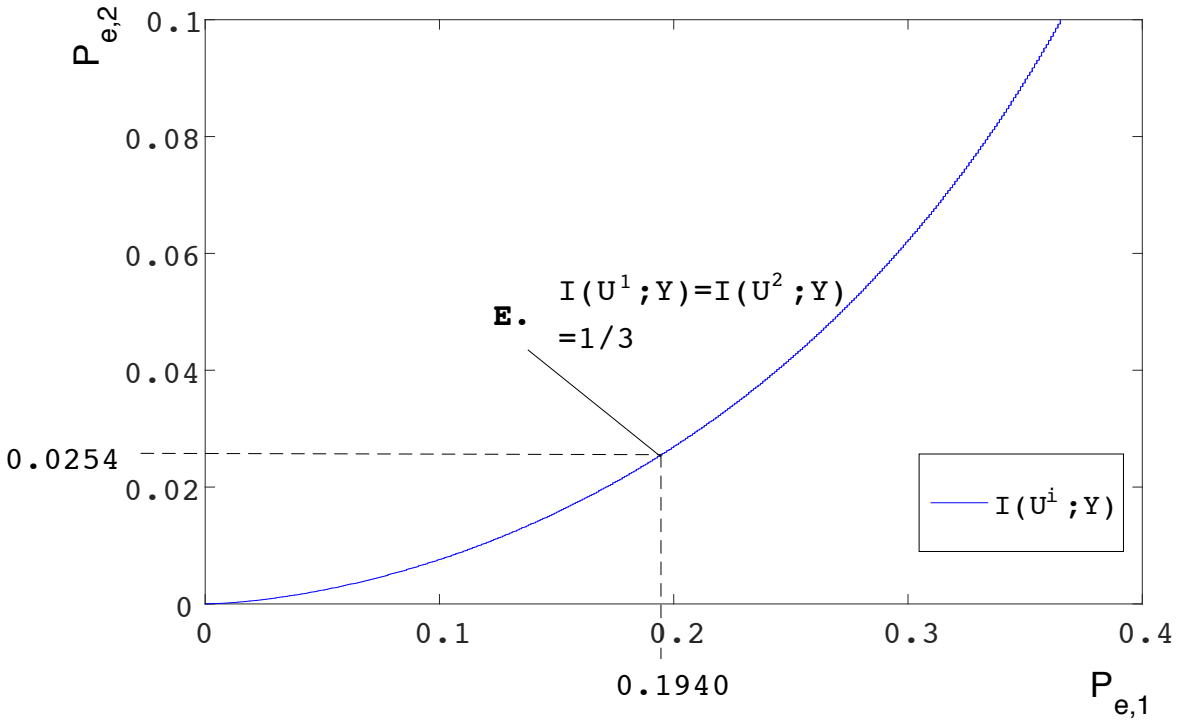

Fig. 6.4 Pairs of $(P_{e,1},\ P_{e,2})$ such that $I(U^1; \mathbf{Y}) = I(U^2; \mathbf{Y})$.

Chapter 7

Relay Channel

The relay channel defined [1] is a channel in which there is one sender and one receiver with a number of intermediate nodes that act as relays to help the communication from the sender to the receiver. This chapter shows an application of our work to practical communications.

7.1 Relay Channel

The relay channel is a kind of channel where there is one source and one destination, however one or more intermediate sender-receiver pairs that act as relays to facilitate the communication between the source and the destination. We mainly treat three-terminal relay channel, which has three-nodes, denoted source (S), relay (R), and destination (D), which is illustrated in Fig.7.1. The relay channel combines a broadcast channel ((S) to (R) and (D)) and a multiple-access channel ((S) and (R) to (D)).

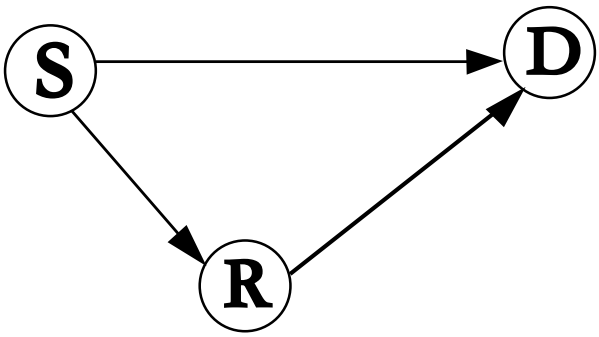

Fig. 7.1 Relay channel.

7.2 Relay channel using WOM codes

This section describes block Markov coding for the relay channel [13], using WOM for AMAC as pictured in Fig. 7.2. The purpose of this section is to demonstrate the usefulness of the AMAC model for the relay channel. In this three-nodes model, the source transmits a message to the destination with the assistance of the relay.

In block Markov coding, there are b transmission blocks, each consisting of n channel uses. A sequence of $(b-1)$ messages M_j, $j \in [1 : b-1]$ are encoded and sent in these b blocks.

The source's message is broadcast to both the relay and the destination. The relay and the source transmit to the destination using a multiple access channel.

A practical transmission scheme using the relay channel with WOM codes, is described as follows: At the first block transmission, the message M_1 in block 1 is encoded into $X_1^1, X_2^1, .., X_n^1$ from codebook C^1, and broadcasted to both the relay and the destination. And the relay is silent. Then, for blocks $j = 2, .., b-1$, the following steps are performed recursively:

1. At the end of block $j-1$, the relay finds the message M_{j-1}.
2. The source is aware of the previous message M_{j-1}, and encodes M_j in block j to $\{X_1^2, X_2^2, .., X_n^2\}$ from codebook C^2, then transmits to the relay and the destination.
3. Simultaneously, the relay having already recovered message M_{j-1}, encodes it to $X_1^1, X_2^1, ..X_n^1$ using C^1, and retransmits it to the destination.
4. The destination receives two codewords $X_1^1 X_2^1 ... X_n^1$ (from block $j-1$) and $X_1^2 X_2^2 ... X_n^2$ (from block j) through a multiple access channel, and decodes as on the AMAC channel.

Here, the source corresponds to User 2, and the relay corresponds to User 1 in the AMAC because the source knows both message M_{j-1} and M_j (i.e. User 2 knows User 1's message); therefore, the proposed WOM codes for the AMAC can be applied to the relay channel with block Markov coding.

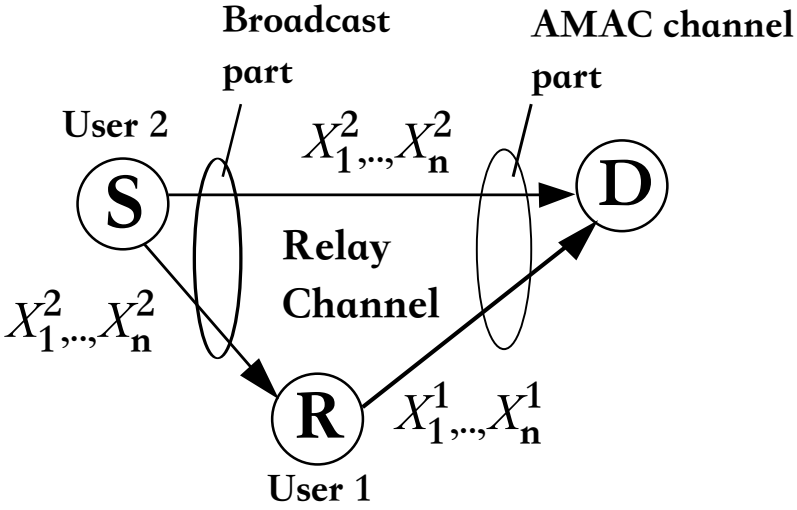

Fig. 7.2 Relay channel using WOM codes. The source (s) plays the role of User 1 in the AMAC, since it knows the relay's message in block Markov scheme.

Chapter 8

Conclusion

8.1 Conclusion

We showed that WOM codes can be applied to the BS-AMAC despite the fact that WOM codes are not designed for wireless communications. Our proposed scheme efficiently separates the two codewords, and avoids the complexities of successive interference cancellation [1] or joint iterative decoding of two codes [8]. Our two low-complexity decoding schemes in cooperative wireless communications are surprisingly effective even in the case with errors. WOM codes change the input distribution from uniform to one suitable for the BS-AMAC channel. Not all rates are achievable by uniform input distributions. However, long WOM codes may not be practical.

We applied a DVB-S.2 LDPC code to our scheme in order to approach the BS-AMAC capacity. Both user's BER performance is below 10^{-6} at $(P_{e,1}, P_{e,2}) = (0.1320, 0.0120)$. Increasing of error probability $P_{e,1}$ is more acceptable in our scheme. This is because of the property of the BS-AMAC in which User 1 message is known to User 2. However, there was the gap in BSC error probabilities $(P_{e,1}, P_{e,2})$ in Fig.6.3, meaning that a LDPC code used in our work is incomplete for our system. Thus, we need to apply other capacity approaching codes, such as polar codes introduced by Arikan [19].

8.2 Future Work

This section describes future works of our research as follows:

1. The *bonus region* refers to achieving rates greater than 1, which is the region (b) pictured in Fig.8.1. Applying WOM codes to the BS-AMAC cannot achieve this region for binary inputs X^1 and X^2. Thus, we propose two encoding schemes for achieving the BS-AMAC rates in the bonus region.

   The first idea is a technique of non-linear mapping of symbols for User 1 with an extended alphabets $u^1 = \{0, 1, 2\}$. Mapping symbols $0, 1 \in U^1$ to $0 \in \mathcal{X}^1$ and $2 \in U^1$ to $1 \in \mathcal{X}^1$ in codewords.

   The second idea is to divide User 1 message into two parts, then encode each part by each user's encoder. Moreover, User 2 sends at a low rate, perhaps 0. Let us show an example pictured in Fig. 8.2, User 1 chooses an index U^1 uniformly from the set $\{0, 1, ..., 15\}$. The length of User 1 message $k = 4$. Since, this message is known to

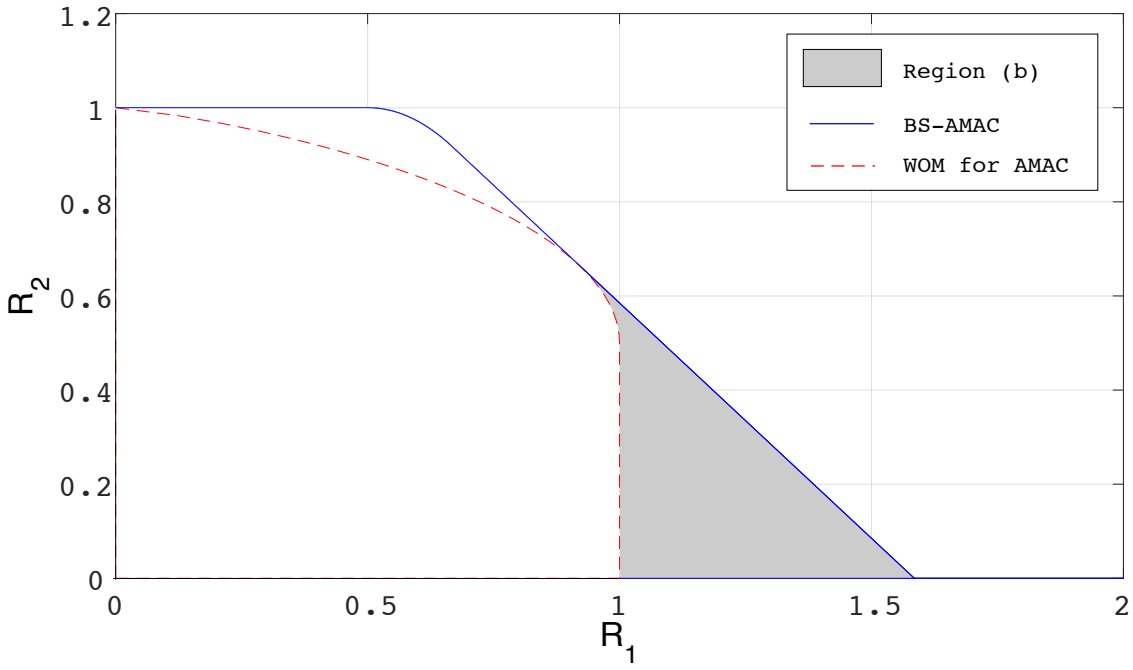

Fig. 8.1 Bonus region (for error free case $P_e = 0$).

both encoders in the AMAC, the first two bits of User 1 message are encoded into X^1 by Encoder 1, and the second two bits are encoded into X^2 by Encoder 2. Note that User 2 does not send any information in this encoding scheme. In this case, User 1 message with length $k = 4$ is encoded into two codewords with length $n = 3$, i.e. this coding scheme achieves a rate pair $(R_1, R_2) = (4/3, 0)$ in the bonus region.

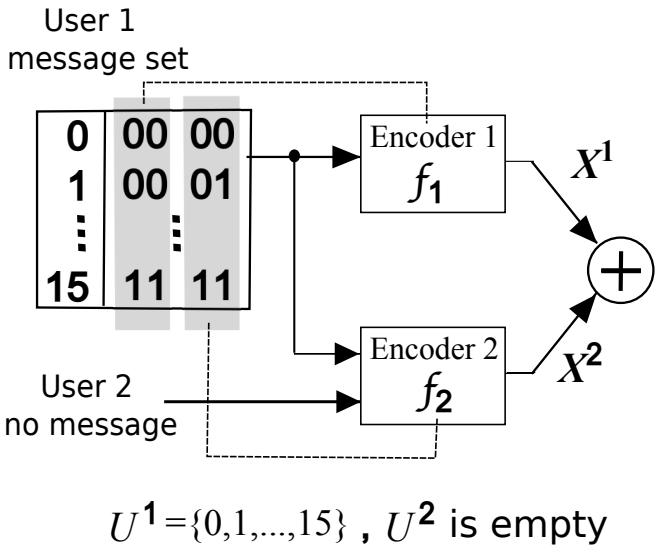

Fig. 8.2 An encoding example achieving a BS-AMAC rate in the bonus region

2. The DVB-S.2 LDPC code used in our work could not approach the BS-AMAC capacity. One possibility to approach the BS-AMAC capacity is by applying polar codes, which were first introduced by Arikan [19]. There are some past works, which are applying polar codes to the asymmetric memoryless channel [20] and combining WOM codes with polar codes called *Polar WOM codes* [21]. We expect that combinations of these schemes will be very effective for our problem.
3. In our research, we assumed a two-user AMAC. However, there may be multiple senders and receivers in practical MAC model. Hence, we need to extend our idea to a multiple user model.

Bibliography

[1] T. M. Cover and J. A. Thomas, *Elements of Information Theory*, 2nd edition, Wiley, 2006.

[2] E. Haroutunian. "Lower bound for the error probability of multiple-access channels", *Problemy Predachi Infromastsii* vol. 11, no. 2, pp. 23-36, 1975.

[3] K. De Bruyn, V. V. Prelov, and E. C. Van Der Meulen, "Reliable Transmission of Two Correlated Sources over an Asymmetric Multiple-Access Channel", *IEEE Transactions on Information Theory*, vol. 33, no. 5, pp. 716-718, 1987.

[4] T. Cover, A. E. Gamal, and M. Salehi, "Multiple access channels with arbitrarily correlated sources", *IEEE Transactions on Information Theory*, vol. 26, no. 6, pp. 648-657, 1980.

[5] D. Gunduz, and E. Erkip, "Correlated sources over an asymmetric multiple access channel with one distortion criterion", in *Proceeding 45th Annual Allerton Conference on Communication, Control and Computing*, (Monticello, IL, USA), pp. 325-330, 2007.

[6] R. L. Rivest and A. Shamir. "How to reuse a 'Write-Once' Memory", *Information and Control*, vol. 55. pp.. 1-19, 1982.

[7] A. Jiang, Y. Li, E. E. Gad, M. Langberg, and J. Bruck, "Joint Rewriting and Error Correction in Write-Once Memory",*Information Theory, IEEE international Symposium on*, pp. 1067-1071, 2013.

[8] Roumy A. and D. Declercq, "Characterization and Optimization of LDPC Codes for the 2-User Gaussian Multiple Access Channel", *EUEASIP Journal on Wireless Communication and Networking*, Article ID: 74890, 2007.

[9] E. Sharon and I. Alrod, "Coding Scheme for Optimizing Random I/O Performance", *Non-Volatile Memory Workshop (NVMW)*, San Diego, USA, Mar. 2013, <http://arxiv.org/abs/1202.6481.pdf>.

[10] G. D. Cohen, P. Godlewski, and F. Merkx, "Linear Binary Code for Write-Once Memories", *IEEE Trans. Inf. Theory*, vol. IT-32, no. 5, pp. 697-700, Oct. 1986.

[11] E. Yaakobi, S. Kayser, P. H. Siegel, A. Vardy and J. K. Wolf. "Codes for Write-Once Memories", *IEEE Trans. on Inf. Theory*, vol. 58, no. 9, pp. 5985-5999, Sep. 2012.

[12] C. Heegard, "On the Capacity of Permanent Memory", *IEEE Trans. on Inf. Theory*, vol. IT-31, no. 1, pp. 34-42, Jan. 1985.

[13] A. E. Gamal, and Y. H. Kim, *Network Information Theory*, Cambridge University Press, 2012.

[14] Y. Wu, "Low complexity codes for writing write-once memory twice", *in Proc. IEEE Int. Symp. Inf. Theory, Austin, TX*, pp. 1928-1932, Jun. 2010.

[15] R. G. Gallager, "Low-Density Parity-Check Codes. Cambridge", MA: MIT, Press, 1963.

[16] A. Neubauer, J. Freudenberger, V. Kuhn, *Coding Theory Algorithms, Architectures and Applications*, Wiley, 2007.

[17] Z. Xiaojie, "LDPC codes : structural analysis and decoding techniques", UC San Diego

Electronic Theses and Dissertations, 2012.

[18] European Telecommunications Standards Institute. Digital video broadcasting (DVB) second generation framing structure, channel coding and modulation systems for broadcasting, interactive services, news gathering and other broadband satellite applications, DRAFT EN 302 307 DVBS2-74r15, 2003.

[19] E. Ariakn, ”Channel polarization: A method for constructing capacity-achieving codes for symmetric binary-input symbol memoryless channels”, *IEEE Transactions on Information Theory*, vol. 55, no. 7, pp. 3051-3073, 2009.

[20] J. Honda and H. Yamamoto, “Polar coding without alphabet extension for asymmetric models”, *Information Theory, IEEE Transactions on*, vol. 59, no. 12, pp. 7829-7838, 2013.

[21] D. Burshtein and A. Strugatski, “Polar write once memory codes”, *IEEE Information Symposium on Information Theory Proceedings*, pp. 1972 -1976, 2012.